# Revised Triple Sampling X Control Charts for the Mean with Known and Estimated Process Parameters

Faijun Nahar Mim, Michael Khoo, Sajal Saha, Philippe Castagliola

# Revised Triple Sampling $\bar{X}$ Control Charts for the Mean with Known and Estimated Process Parameters

Faijun Nahar Mim
School of Mathematical Sciences,
Universiti Sains Malaysia,
11800 Minden, Penang, Malaysia
faijun2005@yahoo.com

Michael B. C. Khoo
School of Mathematical Sciences,
Universiti Sains Malaysia,
11800 Minden, Penang, Malaysia
mkbc@usm.my

Sajal Saha
Department of Mathematics,
International University of Business Agriculture and Technology,
1230 Dhaka, Bangladesh
sajal.saha@iubat.edu

Philippe Castagliola
Université de Nantes & LS2N UMR CNRS 6004,
Nantes, France
philippe.castagliola@univ-nantes.fr

# Revised Triple Sampling $\bar{X}$ Control Charts for the Mean with Known and Estimated Process Parameters


## Abstract

The primary aim of this research is to propose a revised triple sampling (TS) $\bar{X}$ chart, where the derivations of new formulae for computing the average run length of the triple sampling (TS) $\bar{X}$ chart correctly are provided. The secondary aim is to develop the revised TS $\bar{X}$ chart with estimated process parameters. The revised TS $\bar{X}$ charts are compared with the double sampling (DS) $\bar{X}$, two stage adaptive sample size ($AS_2$) $\bar{X}$ and three stage adaptive sample size ($AS_3$ ) $\bar{X}$ charts when process parameters are known and estimated using the average run length (ARL), average number of observations to signal (ANOS), average of the average run lengths (AARL), standard deviation of the average run lengths (SDARL), average of the average number of observations to signal (AANOS) and standard deviation of the average number of observations to signal (SDANOS) criteria, where the revised TS $\bar{X}$ charts are found to be superior. Additionally, a table giving the minimum number of Phase-I samples for estimating the process mean so that the revised TS $\bar{X}$ chart with estimated process parameters has the desired in-control AARL and AANOS performances is provided.



## Keywords

control charts; triple sampling; double sampling; known process parameters; estimated process parameters


## 1. Introduction

An efficient operation of manufacturing processes is considered as one of the key elements that ensure product quality and process efficiency. The real challenge faced by a manufacturing company is to comprehensively consider the major factors that influence the production process, as well as to improve the process quality during the manufacturing process. To avoid unintended deviations from production design and operations, the process fault identification and diagnosis has always been a top priority by management. A quick detection and recognition of such irregularities in a manufacturing process will provide operators with the information they need to make the best decision about the state of a process, thereby achieving the goals of attaining improved product quality, increased product output and lowering manufacturing costs. The study in this article is connected to the aforementioned real-life problem by presenting the revised TS $\bar{X}$ chart, as a control chart is the most effective tool in Statistical Process Control employed in manufacturing companies to detect process irregularities as early as possible so that the necessary corrective actions can be taken immediately, in order to avoid a large number of defective products from being manufactured.

Over the years, numerous enhancements and extensions have been made on different types of control charts, for example, see De la Torre Gutiérrez and Pham (2018); Qu et al. (2018a); Qu et al. (2018b); Abbasi and Haq (2019); Stankus and Castillo-Villar (2019); Li, Wang, and Zhu (2019); Krupskii et al. (2020); Haridy et al. (2020); Wang and Tsung (2020); Celano and Chakraborti (2020); and Hou and Yu (2021); to name some of the recent ones.

A production process can be monitored by adopting an appropriate control chart for a quick detection of process shifts from the nominal operating condition. Different types of control charts have been investigated in the literature, among them are the adaptive control charts, such as the variable sampling interval (VSI) (Reynolds et al., 1988; Guo and Wang, 2016), variable sample size (Prabhu, Runger and Keats, 1993; Costa, 1994; Zimmer, Montgomery and Runger, 1998; Aparisi et al., 2014) and variable parameters (Costa, 1999) charts.

A type of adaptive charts that has received a great deal of attention among researchers are the DS charts. The DS control charting technique based on the sample mean $\bar{X}$ was pioneered by Croasdale (1974), where a decision about the status of a process (in-control or out-of-control) depends on the information from the second sample only. Daudin (1992) modified Croasdale's DS $\bar{X}$ control charting procedure, where the new DS $\bar{X}$ chart uses the information from either the first sample or combined samples in deciding about the status of the process. Irianto and Shinozaki (1998) presented an optimal design procedure for the DS $\bar{X}$ chart, where the power of the chart in detecting shifts is maximized, instead of minimizing the average sample size for small shifts as advised by Daudin (1992). The more recent studies on charts using the DS technique were made Costa (2017); Haq and Khoo (2018); and Huang, Yang, and Xie (2020).

In the literature, the DS control charting procedure is combined with another control chart at hand in the development of a more advanced chart. Carot, Jabaloyes and Carot (2002) investigated the combined DS and VSI $\bar{X}$ charts. Khoo et al. (2010) combined the DS and synthetic control charting procedures and introduced the synthetic DS $\bar{X}$ chart for monitoring the process mean. Khoo et al. (2015) merged the DS and side sensitive group runs (SSGR) charting techniques to propose the SSGRDS $\bar{X}$ chart and showed that this new chart performs better than the SSGR $\bar{X}$ chart. Subsequently, Saha et al. (2018) incorporated the side sensitive modified group runs (SSMGR) approach into the DS chart in developing the SSMGRDS $\bar{X}$ chart.

With the aim of increasing the sensitivity of the DS $\bar{X}$ chart in detecting mean shifts, He, Grigoryan, and Sigh (2002) proposed the triple sampling (TS) $\bar{X}$ chart, where the latter uses either the first, combined first and second, or combined first, second and third samples in deciding about the status of a process. They showed that the TS $\bar{X}$ chart is more efficient than the DS $\bar{X}$ chart in minimizing the average sample size (ASS) when the process is in-control.

Hsu (2004) claimed that the conclusion made by He, Grigoryan and Sigh (2002) is controversial as the out-of-control ASS is not taken into account in comparing the efficiency of the TS $\bar{X}$ and DS $\bar{X}$ charts.

Control charts are usually designed by assuming that the process parameters are known. However, in practice, in most process monitoring situations, the process parameters are usually unknown and need to be estimated from an in-control Phase-I dataset or historical data. When the unknown parameters are replaced by their estimates, the performance of the control chart is significantly different from its known process parameters counterpart. Researches on the effects of parameter estimation on the efficiency of various types of control charts are actively being conducted in recent years. Recent researches on the estimation of process parameters on control charts include Faraz, Woodall, and Heuchenne (2015); Hu et al. (2018); Aparisi, Mosquera, and Epprecht (2018); Faraz, Heuchenne, and Saniga (2018); Saha et al. (2019); and Hu and Castagliola (2019); to name some. Accurate estimations of process parameters in Phase-I is crucial for the computation of reliable control limits in monitoring a Phase-II process, which explains why so much attention is given to researches on the various charts with estimated process parameters.

Most of the earlier researches on DS charts in the literature assume that process parameters are known. The DS $\bar{X}$ chart with estimated process parameters was introduced by Khoo et al. (2013), where three different optimal designs were presented. You et al. (2015) proposed the synthetic DS $\bar{X}$ chart with estimated process parameters by suggesting an adequate number of Phase-I samples to estimate the process parameters in order to have approximately the same in-control performance as the corresponding chart's known process parameters counterpart. Meanwhile, the design of the DS $S^2$ chart with estimated process variance and its statistical properties for evaluating the efficiency of the chart in monitoring the variance were given by

Castagliola, Oprime, and Khoo (2017). More recent studies on the DS charts with estimated process parameters were made by Lee and Khoo (2019); and Motsepa et al. (2020).

In relation to the TS $\bar{X}$ chart, Hsu (2004) encountered problems in computing the chart's Type-II error rate using the mathematical model in He, Grigoryan and Sigh (2002) as no output was generated by the Mathematica program that he employed. To date, the error in the mathematical model of the TS $\bar{X}$ chart in He, Grigoryan and Sigh (2002) has not been pointed out by researchers in the literature. Furthermore, even though the impact of parameter estimation on control charts has been extensively developed in the literature, the TS $\bar{X}$ chart with estimated process parameters still does not exist in the literature. In view of these setbacks, two major research perspectives have been advocated in this paper. Firstly, the oversight in the mathematical model of He, Grigoryan and Sigh (2002) will be pointed out, where corrections to rectify this oversight will be provided in the form of the proposed revised TS $\bar{X}$ chart. Numerical analysis will be conducted to illustrate the problem in the mathematical model of He, Grigoryan and Sigh (2002). Secondly, the revised TS $\bar{X}$ chart with estimated process parameters will be developed. The recommended minimum number of Phase-I samples required in the estimation of process parameters so that the revised TS $\bar{X}$ chart with estimated process parameters has an in-control AANOS (or AARL) performance that is close to that of the chart's known process parameters counterpart will be given.

The contribution of this study involves providing optimal parameters of the revised TS $\bar{X}$ chart with known process parameters in minimizing the out-of-control ARL ($\mathrm{ARL}(\delta)$) and ANOS ($\mathrm{ANOS}(\delta)$) values, and that of the revised TS $\bar{X}$ chart with estimated process parameters in minimizing the out-of-control AARL ($\mathrm{AARL}(\delta)$) and AANOS ($\mathrm{AANOS}(\delta)$) values, for various sizes of process mean shifts, $\delta$ (> 0). The ARL and ANOS criteria are used in evaluating the performance of the revised TS $\bar{X}$ chart with known process parameters, while the AARL, SDARL, AANOS and SDANOS criteria are employed in evaluating the estimated process

parameters based revised TS $\bar{X}$ chart. An illustrative example using a real dataset on flow width measurements from the production system is given to explain the design and implementation procedure of the new revised TS $\bar{X}$ chart with estimated process parameters. The inclusion of process parameter estimation in the design and implementation of the estimated process parameters based revised TS $\bar{X}$ chart and evaluation of the chart's performances using the AARL, SDARL, AANOS and SDANOS criteria constitute the innovative contribution of this study. Prior to this study, the design of the TS $\bar{X}$ chart in the literature is only confined to situations with known process parameters.

The remainder of this manuscript is organized as follows: Section 2 discusses the TS $\bar{X}$ chart of He, Grigoryan, and Sigh (2002). Section 3 entails the new mathematical model with the correct formulae for the design of the revised TS $\bar{X}$ chart, where the erroneous formulae in He, Grigoryan, and Sigh (2002) are pointed out. The statistical properties and correct formulae in computing the performance measures of the known and estimated process parameters based revised TS $\bar{X}$ charts are elaborated in this section. In Section 4, the optimal designs of the revised TS $\bar{X}$ chart with known and estimated process parameters are presented. Section 5 provides numerical results for the performance comparisons of the following charts when process parameters are known: (i) revised TS $\bar{X}$, (ii) DS $\bar{X}$, (iii) two stage adaptive sample size ($AS_2$ $\bar{X}$) and (iv) three stage adaptive sample size ($AS_3$ $\bar{X}$) charts. Additionally, when process parameters are estimated, the revised TS $\bar{X}$ chart is compared with the DS $\bar{X}$ chart. In addition, the required minimum number of Phase-I samples to estimate the process parameters so that the AANOS(0) and AARL(0) performances of the estimated process parameters based revised TS $\bar{X}$ chart is close to the ANOS(0) and ARL(0) performances of the revised TS $\bar{X}$ chart with known process parameters, respectively, are given. Section 6 illustrates the implementation of the revised TS $\bar{X}$ chart with estimated process parameters using data from a hard bake process. Finally, concluding remarks are drawn and future researches are suggested in Section 7.

## 2. The revised TS $\bar{X}$ chart

Assume that the quality characteristic, $X$ follows a normal distribution, where the in-control population mean and standard deviation are denoted as $\mu_0$ and $\sigma_0$, respectively. The process being monitored will become out-of-control when the process mean shifts from $\mu_0$ to $\mu_0 - \delta\sigma_0$, where it is assumed that the process standard deviation remains unchanged and $\delta$ is the size of the standardized process mean shift. It is shown in Figure 1 that the revised TS $\bar{X}$ chart has three levels of inspections. The warning and control limits in level 1 are $\pm L_{11}$ and $\pm L_{12}$, respectively, while that for level 2 are $\pm L_{21}$ and $\pm L_{22}$, respectively, and the control limits in level 3 are $\pm L_3$. Note that $L_{12} > L_{11}$ and $L_{22} > L_{21}$. All the limits in the revised TS $\bar{X}$ chart are referred to as standardized limits. The sample sizes for the first, second and third samples are denoted as $n_1$, $n_2$ and $n_3$, respectively. Let $X_{li,j}$ denote the $j^{\text{th}}$ observation of inspection level $l$ at sampling stage $i$, where $j = 1, 2, \ldots, n_l$ and $l = 1$, 2 or 3. By referring to Figure 1, the revised TS $\bar{X}$ chart is implemented as follows:

Insert Figure 1 here

Step 1. Determine the limits $L_{11}$, $L_{12}$, $L_{21}$, $L_{22}$ and $L_3$.

Step 2. At sampling stage $i$, take an initial sample of size $n_1$ (inspection level 1) and compute the sample mean $\bar{X}_{1i} = \dfrac{1}{n_1}\sum_{j=1}^{n_1} X_{1i,j}$.

Step 3. Let $Y_{1i} = \bar{X}_{1i}$ and compute $W_{1i} = \dfrac{(Y_{1i} - \mu_0)\sqrt{n_1}}{\sigma_0}$. If $W_{1i} \in I_{11} = [-L_{11}, L_{11}]$, the process is in-control and the control flow returns to Step 2.

Step 4. If $W_{1i} \in I_{13} = (-\infty, -L_{12}) \cup (L_{12}, +\infty)$, the process is out-of-control and the control flow proceeds to Step 11.

Step 5. If $W_{1i} \in I_{12} = [-L_{12}, -L_{11}) \cup (L_{11}, L_{12}]$, take a second sample of size $n_2$ (inspection level 2) and compute the mean of the second sample $\bar{X}_{2i} = \frac{1}{n_2}\sum_{j=1}^{n_2} X_{2i,j}$. Then compute the combined sample mean of the first and second samples $Y_{2i} = \frac{n_1\bar{X}_{1i} + n_2\bar{X}_{2i}}{n_1 + n_2}$, followed by $W_{2i} = \frac{(Y_{2i} - \mu_0)\sqrt{n_1 + n_2}}{\sigma_0}$.

Step 6. If $W_{2i} \in I_{21} = [-L_{21}, L_{21}]$, the process is in-control and the control flow returns to Step 2.

Step 7. If $W_{2i} \in I_{23} = (-\infty, -L_{22}) \cup (L_{22}, +\infty)$, the process is out-of-control and the control flow proceeds to Step 11.

Step 8. If $W_{2i} \in I_{22} = [-L_{22}, -L_{21}) \cup (L_{21}, L_{22}]$, take a third sample of size $n_3$ (inspection level 3). Compute the mean of the third sample $\bar{X}_{3i} = \frac{1}{n_3}\sum_{j=1}^{n_3} X_{3i,j}$, followed by the combined sample mean of the first, second and third samples $Y_{3i} = \frac{n_1\bar{X}_{1i} + n_2\bar{X}_{2i} + n_3\bar{X}_{3i}}{n_1 + n_2 + n_3}$ and $W_{3i} = \frac{(Y_{3i} - \mu_0)\sqrt{n_1 + n_2 + n_3}}{\sigma_0}$.

Step 9. If $W_{3i} \in I_3 = [-L_3, L_3]$, the process is in-control and the control flow returns to Step 2.

Step 10. If $W_{3i} \notin I_3$, the process is out-of-control and the control flow proceeds to Step 11.

Step 11. An out-of-control is signaled at sampling stage *i* and corrective actions are needed to investigate and remove the assignable cause(s). Then return to Step 2.

Table 1 gives a summary of the statistics used in the 11 steps procedure and their distributions.

Insert Table 1 here

## 3. Properties of the revised TS $\bar{X}$ chart with known and estimated process parameters

This section consists of two subsections. The statistical properties of the revised TS $\bar{X}$ chart with known process parameters (called the revised TS$_K$ $\bar{X}$ chart, hereafter) are explained in Section 3.1, while the revised TS $\bar{X}$ chart with estimated process parameters (called the revised TS$_E$ $\bar{X}$ chart, hereafter) are discussed in Section 3.2.

### *3.1. Properties of the revised TS$_K$ $\bar{X}$ chart*

Let $P_a$ represent the probability of declaring the process as in-control and $P_{al}$ is the probability of declaring the process as in-control at inspection level *l*, for *l* = 1, 2 and 3. Thus,

$$P_a = P_{a1} + P_{a2} + P_{a3}. \tag{1}$$

The formulae for computing $P_{al}$, for *l* = 1, 2 and 3 are explained in the discussion that follows. As pointed out by Daudin (1992), the probability that the process is declared as in-control at inspection level 1 is

$$P_{a1} = \Pr\left(W_{1i} \in I_{11}\right) = \Phi\left(L_{11} + \delta\sqrt{n_1}\right) - \Phi\left(-L_{11} + \delta\sqrt{n_1}\right), \tag{2}$$

while the probability that the process is declared as in-control at inspection level 2 is

$$P_{a2} = \int_{w_1 \in I_{12}} \Pr\left[W_{2i} \in I_{21} \middle| W_{1i} = w_1\right] f_{W_{1i}}\left(w_1\right) \mathrm{d}w_1$$

$$= \int_{z_1' \in I_{12}^*} \left[\Phi\left(c_2 L_{21} + r_2 c_2 \delta - z_1' \sqrt{\frac{n_1}{n_2}}\right) - \Phi\left(-c_2 L_{21} + r_2 c_2 \delta - z_1' \sqrt{\frac{n_1}{n_2}}\right)\right] \phi\left(z_1'\right) \mathrm{d}z_1', \tag{3}$$

where $z_1' = \sqrt{n_1}\left(\bar{x}_{1i} - \mu_0 + \delta\sigma_0\right)/\sigma_0$, $r_2 = \sqrt{n_1 + n_2}$, $c_2 = \sqrt{\dfrac{n_1 + n_2}{n_2}}$, $I_{12}^* = \left[-L_{12} + \delta\sqrt{n_1}, -L_{11} + \delta\sqrt{n_1}\right] \cup \left[L_{11} + \delta\sqrt{n_1}, L_{12} + \delta\sqrt{n_1}\right]$ and $\phi(\cdot)$ and $\Phi(\cdot)$ are the standard normal probability density function (pdf) and distribution function, respectively.

In He, Grigoryan, and Sigh (2002), the probability of declaring the process as in-control at inspection level 3 is $P_{a3} = \int_{x \in I_{12}'} \int_{y \in I_{22}'} \Pr\left[Y_{3i} \in I_3' \middle| Y_{2i} = y \text{ and } \bar{X}_{1i} = x\right] f_{Y_{2i}}\left(y\right) f_{\bar{X}_{1i}}\left(x\right) \mathrm{d}y\mathrm{d}x$

$$= \int_{z_1' \in I_{12}^*} \int_{z_2' \in I_{22}''} \left[ \Phi\left( c_3 L_3 + r_3 c_2 \delta - z_1' \sqrt{\frac{n_1}{n_3}} - z_2' \sqrt{\frac{n_2}{n_3}} \right) - \Phi\left( -c_3 L_3 + r_3 c_3 \delta - z_1' \sqrt{\frac{n_1}{n_3}} - z_2' \sqrt{\frac{n_2}{n_3}} \right) \right] \times \phi(z_1') \phi(z_2') \mathrm{d}z_2' \mathrm{d}z_1', \tag{4}$$

where

$$I_{12}' = \left[ \mu_0 - \frac{L_{12}\sigma_0}{\sqrt{n_1}}, \mu_0 - \frac{L_{11}\sigma_0}{\sqrt{n_1}} \right] \cup \left[ \mu_0 + \frac{L_{11}\sigma_0}{\sqrt{n_1}}, \mu_0 + \frac{L_{12}\sigma_0}{\sqrt{n_1}} \right],$$

$$I_{22}' = \left[ \mu_0 - \frac{L_{22}\sigma_0}{\sqrt{n_1+n_2}}, \mu_0 - \frac{L_{21}\sigma_0}{\sqrt{n_1+n_2}} \right] \cup \left[ \mu_0 + \frac{L_{21}\sigma_0}{\sqrt{n_1+n_2}}, \mu_0 + \frac{L_{22}\sigma_0}{\sqrt{n_1+n_2}} \right],$$

$$I_3' = \left[ \mu_0 - \frac{L_3\sigma_0}{\sqrt{n_1+n_2+n_3}}, \mu_0 + \frac{L_3\sigma_0}{\sqrt{n_1+n_2+n_3}} \right], \qquad I_{22}'' = \left[ -L_{22} + \delta\sqrt{n_1+n_2}, -L_{21} + \delta\sqrt{n_1+n_2} \right] \cup$$

$\left[ L_{21} + \delta\sqrt{n_1+n_2}, L_{22} + \delta\sqrt{n_1+n_2} \right]$, while $f_{Y_{2i}}(y)$ and $f_{\bar{X}_{1i}}(x)$ are the pdfs of $Y_{2i}$ and $\bar{X}_{1i}$, respectively. The $P_{a3}$ formula in Equation (4) is not correct as the random variables $Y_{2i}$ and $\bar{X}_{1i}$ are not independent and its associated double integral should not contain the product of their pdfs, i.e. $f_{Y_{2i}}(y)$ and $f_{\bar{X}_{1i}}(x)$ (as if $Y_{2i}$ and $\bar{X}_{1i}$ are independent). Furthermore, the ARL values computed by the authors of this manuscript based on $P_{a3}$ in Equation (4) are significantly different from those obtained by simulation.

At sampling stage *i*, the probability that the process is in-control at inspection level 3 (i.e. $P_{a3}$) is equal to the probability that $W_{3i}$ falls in interval $I_3$, given that $W_{2i}$ and $W_{1i}$ fall in interval $I_{22}$ at inspection level 2 and in interval $I_{12}$ at inspection level 1, respectively.

Then, asserting that $W_{1i} \in I_{12}$ is equivalent to saying that $Z_{1i}' = \sqrt{n_1}\left(\bar{X}_{1i} - \mu_0 + \delta\sigma_0\right)/\sigma_0 \in I_{12}^*$, where $I_{12}^*$ has been defined in Equation (3). The

mathematical derivation to show that $W_{1i} \in I_{12}$ is equivalent to $Z'_{1i} \in I^*_{12}$ is given in Appendix A.1.

In addition, condition on $Z'_{1i} = z'_1$, asserting that $W_{2i} \in I_{22}$ is equivalent to saying that $Z'_{2i} = \sqrt{n_2}\left(\bar{X}_{2i} - \mu_0 + \delta\sigma_0\right)\big/\sigma_0 \in I^*_{22}$ (see Appendix A.2), where

$$I^*_{22} = \left[-c_2 L_{22} + r_2 c_2 \delta - z'_1\sqrt{\frac{n_1}{n_2}}, -c_2 L_{21} + r_2 c_2 \delta - z'_1\sqrt{\frac{n_1}{n_2}}\right] \cup \left[c_2 L_{21} + r_2 c_2 \delta - z'_1\sqrt{\frac{n_1}{n_2}}, c_2 L_{22} + r_2 c_2 \delta - z'_1\sqrt{\frac{n_1}{n_2}}\right].$$

Similarly, condition on $Z'_{1i} = z'_1$ and $Z'_{2i} = z'_2$, asserting that $W_{3i} \in I_3$ is equivalent to saying that $Z'_{3i} = \sqrt{n_3}\left(\bar{X}_{3i} - \mu_0 + \delta\sigma_0\right)\big/\sigma_0 \in I^*_3$ (see Appendix A.3), where

$$I^*_3 = \left[-c_3 L_3 + r_3 c_3 \delta - z'_1\sqrt{\frac{n_1}{n_3}} - z'_2\sqrt{\frac{n_2}{n_3}}, c_3 L_3 + r_3 c_3 \delta - z'_1\sqrt{\frac{n_1}{n_3}} - z'_2\sqrt{\frac{n_2}{n_3}}\right].$$

Based on the above discussions, $P_{a3}$ can be written as

$$P_{a3} = \int_{z'_1 \in I^*_{12}} \int_{z'_2 \in I^*_{22}} \Pr\left(Z'_{3i} \in I^*_3\right) f_{Z'_{1i}}\left(z'_1\right) f_{Z'_{2i}}\left(z'_2\right) \mathrm{d}z'_2 \mathrm{d}z'_1$$

$$= \int_{z'_1 \in I^*_{12}} \int_{z'_2 \in I^*_{22}} \left[\Phi\left(c_3 L_3 + r_3 c_3 \delta - z'_1\sqrt{\frac{n_1}{n_3}} - z'_2\sqrt{\frac{n_2}{n_3}}\right) - \right.$$

$$\left. \Phi\left(-c_3 L_3 + r_3 c_3 \delta - z'_1\sqrt{\frac{n_1}{n_3}} - z'_2\sqrt{\frac{n_2}{n_3}}\right)\right] \phi\left(z'_1\right)\phi\left(z'_2\right) dz'_2 dz'_1 . \qquad (5)$$

Note that $I^*_{12}$ and $z'_1$ have been defined in Equation (3), while $I^*_{22}$ has been defined prior to this discussion. The other notations are defined as $z'_2 = \sqrt{n_2}\left(\bar{x}_{2i} - \mu_0 + \delta\sigma_0\right)\big/\sigma_0$, $r_3 = \sqrt{n_1 + n_2 + n_3}$ and $c_3 = \sqrt{\dfrac{n_1 + n_2 + n_3}{n_3}}$. As $Z'_{1i}$ and $Z'_{2i}$ are standard normal random variables, their pdfs can also be written as $f_{Z'_{1i}}\left(z'_1\right) = \phi\left(z'_1\right)$ and $f'_{Z_{2i}}\left(z'_1\right) = \phi\left(z'_2\right)$, respectively. The problem raised in Equation (4) no longer exists as $Z'_{1i}$ and $Z'_{2i}$ are by definitions independent and using the product of their pdfs as in Equation (5) now makes sense.

Table 2 shows the ARL(0) values of the (i) $TS_K$ $\bar{X}$ chart adopted from He, Grigoryan, and Sigh (2002), (ii) revised $TS_K$ $\bar{X}$ chart computed using MATLAB based on the model proposed in this section, and (iii) revised $TS_K$ $\bar{X}$ chart simulated using SAS, as well as the 95% confidence interval for ARL(0) of the revised $TS_K$ $\bar{X}$ chart simulated using SAS, all obtained based on the parameters in He, Grigoryan, and Sigh (2002). It is observed that the ARL(0) values of the revised $TS_K$ $\bar{X}$ chart computed using the proposed model are about the same as that simulated. Additionally, the ARL(0) values obtained using the proposed model fall in their corresponding 95% confidence intervals. However, the ARL(0) values adopted from He, Grigoryan, and Sigh (2002) are totally different from the simulated ones and none of them falls in their respective 95% confidence intervals. For example, when the parameter combination $(n_1, n_2, n_3, L_{11}, L_{12}$ $L_{21}, L_{22}, L_3)$ = (2, 2, 1, 1.47, 3.00, 3.30, 1.80, 2.87) is considered, ARL(0) = 181.96 is obtained for the revised $TS_K$ $\bar{X}$ chart using the model proposed in this section, where this ARL(0) value is close to that simulated using SAS (ARL(0) = 182.41). Furthermore, the ARL(0) (= 181.96) value computed based on the proposed model falls in the 95% confidence interval for ARL(0), i.e. (179.15, 184.51). It is obvious that, for this example, the ARL(0) (= 370.40) value reported in He, Grigoryan, and Sigh (2002) is incorrect as it is different from the simulated ARL(0) value of 182.41. Moreover, the ARL(0) (= 370.40) value in He, Grigoryan, and Sigh (2002) does not fall in the corresponding 95% confidence interval for ARL(0), i.e. (179.15, 184.51). The findings explained in this paragraph show that the formula provided by He, Grigoryan, and Sigh (2002) in computing the ARL is incorrect.

Insert Table 2 here

The average sample size (ASS) at sampling stage *i* of the revised $TS_K$ $\bar{X}$ chart is computed as

$$\text{ASS} = n_1 + n_2 P_2 + n_3 P_3, \tag{6}$$

where $P_2$ and $P_3$ denote the probabilities of taking the second and third samples, respectively. Consequently,

$$P_2 = \Pr\left(W_{1i} \in I_{12}\right)$$

$$= \Phi\left(L_{12} + \delta\sqrt{n_1}\right) - \Phi\left(L_{11} + \delta\sqrt{n_1}\right) + \Phi\left(-L_{11} + \delta\sqrt{n_1}\right) - \Phi\left(-L_{12} + \delta\sqrt{n_1}\right), \tag{7}$$

while $P_3 = \Pr\left(W_{2i} \in I_{22} \middle| W_{1i} \in I_{12}\right) = \int_{w_1 \in I_{12}} \Pr\left(W_{2i} \in I_{22} \middle| W_{1i} = w_1\right) f_{W_{1i}}\left(w_1\right) \mathrm{d}w_1$

$$= \int_{z_1' \in I_{12}^*} \left[ \Phi\left( -c_2 L_{21} + r_2 c_2 \delta - z_1' \sqrt{\frac{n_1}{n_2}} \right) - \Phi\left( -c_2 L_{22} + r_2 c_2 \delta - z_1' \sqrt{\frac{n_1}{n_2}} \right) \right] \phi\left(z_1'\right) \mathrm{d}z_1' +$$

$$\int_{z_1' \in I_{12}^*} \left[ \Phi\left( c_2 L_{22} + r_2 c_2 \delta - z_1' \sqrt{\frac{n_1}{n_2}} \right) - \Phi\left( c_2 L_{21} + r_2 c_2 \delta - z_1' \sqrt{\frac{n_1}{n_2}} \right) \right] \phi\left(z_1'\right) \mathrm{d}z_1' . \tag{8}$$

The formula derivation of $P_3$ in Equation (8) is shown in Appendix A.4. A control chart's efficiency is generally measured by the speed in which an out-of-control situation is detected. A common performance criterion that measures this speed is the ARL. As any Shewhart-type control chart, the ARL of the revised TS$_K$ $\bar{X}$ chart is computed as

$$\mathrm{ARL} = \frac{1}{1 - P_a} . \tag{9}$$

In the revised TS control charting technique, the number of observations taken in each sampling stage varies, i.e. either $n_1$, $n_1 + n_2$ or $n_1 + n_2 + n_3$. However, for the DS chart, the number of observations taken in each sampling stage is either $n_1$ or $n_1 + n_2$. Therefore, in comparing the performances between the DS and TS schemes, many researchers suggested the use of the ANOS criterion, instead of relying solely on the ARL criterion (which only measures the average number of sampling stages to signal) because the number of observations taken in each sampling stage for these two schemes is different. The ANOS value of the revised TS$_K$ $\bar{X}$ chart is computed as

$$\mathrm{ANOS} = \mathrm{ARL} \times \mathrm{ASS}$$

$$= \frac{n_1 + n_2 P_2 + n_3 P_3}{1 - P_a}. \tag{10}$$

### *3.2. Properties of the revised $TS_E$ $\bar{X}$ chart*

When the in-control process parameters $\mu_0$ and $\sigma_0$ are unknown, they need to be estimated from an in-control Phase-I dataset that contains *m* samples, each with *n* observations, i.e. $\{T_{i,1}, T_{i,2}, \ldots, T_{i,n}\}$, for $i = 1, 2, \ldots, m$. Assume that independence between and within these *m* samples exists and $T_{i,j} \sim N\left(\mu_0, \sigma_0^2\right)$, for $i = 1, 2, \ldots, m$ and $j = 1, 2, \ldots, n$.

The estimators $\hat{\mu}_0$ and $\hat{\sigma}_0$ of the parameters $\mu_0$ and $\sigma_0$, respectively, are computed as

$$\hat{\mu}_0 = \frac{1}{m}\sum_{i=1}^{m} \bar{T}_i \tag{11}$$

and

$$\hat{\sigma}_0 = \sqrt{\frac{1}{m(n-1)}\sum_{i=1}^{m}\sum_{j=1}^{n}\left(T_{i,j} - \bar{T}_i\right)^2}, \tag{12}$$

where $\bar{T}_i$ is the sample mean of the observations $\{T_{i,1}, T_{i,2}, \ldots, T_{i,n}\}$.

The procedure of implementation of the revised $TS_E$ $\bar{X}$ chart is similar to that of the revised $TS_K$ $\bar{X}$ chart explained in Section 2, except that $W_{1i}$, $W_{2i}$ and $W_{3i}$ in the step-by-step procedure of the aforementioned section are replaced by $\hat{W}_{1i}$, $\hat{W}_{2i}$ and $\hat{W}_{3i}$, respectively. $\hat{W}_{1i}$, $\hat{W}_{2i}$ and $\hat{W}_{3i}$ are computed from the $W_{1i}$, $W_{2i}$ and $W_{3i}$ formulae, respectively, by substituting $\mu_0$ with $\hat{\mu}_0$ and $\sigma_0$ with $\hat{\sigma}_0$. In the revised $TS_E$ $\bar{X}$ chart, the probability of declaring the process as in-control at inspection level *l*, for *l* = 1, 2 and 3, is denoted as $\hat{P}_{al}$. Consequently, the probability that a process is declared as in-control is

$$\hat{P}_a = \hat{P}_{a1} + \hat{P}_{a2} + \hat{P}_{a3}. \tag{13}$$

$\hat{P}_{a1}$ is computed as (Khoo et al. 2013)

$$\hat{P}_{a1} = \Pr\left(\hat{W}_{1i} \in I_{11} \,|\, \hat{\mu}_0, \hat{\sigma}_0\right) = \Phi\left[U\sqrt{\frac{n_1}{mn}} + VL_{11} + \delta\sqrt{n_1}\right] - \Phi\left[U\sqrt{\frac{n_1}{mn}} - VL_{11} + \delta\sqrt{n_1}\right], \qquad (14)$$

where the random variables *U* and *V* are defined as

$$U = \left(\hat{\mu}_0 - \mu_0\right)\frac{\sqrt{mn}}{\sigma_0} \qquad (15)$$

and

$$V = \frac{\hat{\sigma}_0}{\sigma_0}, \qquad (16)$$

respectively. *U* follows the standard normal distribution and $V^2$ follows the gamma distribution with parameters $\left(\frac{m(n-1)}{2}\right)$ and $\left(\frac{2}{m(n-1)}\right)$, i.e. $V^2 \sim \gamma\left(\frac{m(n-1)}{2}, \frac{2}{m(n-1)}\right)$. Then the pdf of *U* and *V* are defined as

$$f_U(u) = \phi(u) \qquad (17)$$

and

$$f_V(v) = 2v\, f_\gamma\left(v^2 \left| \frac{m(n-1)}{2}, \frac{2}{m(n-1)}\right.\right), \qquad (18)$$

respectively, where $f_\gamma(\cdot)$ is the pdf of the gamma distribution with parameters $\frac{m(n-1)}{2}$ and $\frac{2}{m(n-1)}$.

Additionally, $\hat{P}_{a2}$ is computed as (Khoo et al. 2013)

$$\hat{P}_{a2} = \Pr\left(\hat{W}_{2i} \in I_{21} \text{ and } \hat{W}_{1i} \in I_{12} \,\middle|\, \hat{\mu}_0, \hat{\sigma}_0\right)$$

$$= \int_{w_1 \in I_{12}} \left[ \Phi\left( U\sqrt{\frac{n_2}{mn}} + V\left( c_2 L_{21} - w_1\sqrt{\frac{n_1}{n_2}} \right) + \delta\sqrt{n_2} \right) - \right.$$

$$\left. \Phi\left( U\sqrt{\frac{n_2}{mn}} - V\left( c_2 L_{21} + w_1\sqrt{\frac{n_1}{n_2}} \right) + \delta\sqrt{n_2} \right) \right] f_{\hat{W}_{1i}}\left( w_1 \middle| \hat{\mu}_0, \hat{\sigma}_0 \right) \mathrm{d}w_1, \qquad (19)$$

where

$$f_{\hat{W}_{1i}}\left( w_1 \middle| \hat{\mu}_0, \hat{\sigma}_0 \right) = V\phi\left( U\sqrt{\frac{n_1}{mn}} + Vw_1 + \delta\sqrt{n_1} \right). \qquad (20)$$

Note that Equations (14), (19) and (20) are based on the out-of-control mean considered in this manuscript, i.e. $\mu_0 - \delta\sigma_0$.

At sampling stage *i,* the probability that the process is declared as in-control at inspection level 3 (i.e. $\hat{P}_{a3}$) is equal to the probability that $\hat{W}_{3i}$ falls in interval $I_3$, given that $\hat{W}_{2i}$ and $\hat{W}_{1i}$ fall in interval $I_{22}$ at inspection level 2 and in interval $I_{12}$ at inspection level 1, respectively.

Then, condition on $\hat{W}_{1i} = w_1$, asserting that $\hat{W}_{2i} \in I_{22}$ is equivalent to saying that $\hat{Z}_{2i} = \dfrac{\sqrt{n_2}\left( \bar{X}_{2i} - \hat{\mu}_0 \right)}{\hat{\sigma}_0} \in I_{22}^{**}$, where

$$I_{22}^{**} = \left[ -c_2 L_{22} - w_1\sqrt{\frac{n_1}{n_2}},\ -c_2 L_{21} - w_1\sqrt{\frac{n_1}{n_2}} \right] \cup \left[ c_2 L_{21} - w_1\sqrt{\frac{n_1}{n_2}},\ c_2 L_{22} - w_1\sqrt{\frac{n_1}{n_2}} \right].$$

The mathematical derivation to show that $\hat{W}_{2i} \in I_{22}$ is equivalent to $\hat{Z}_{2i} \in I_{22}^{**}$ is given in Appendix B.1.

Similarly, condition on $\hat{W}_{1i} = w_1$ and $\hat{Z}_{2i} = z_2$, asserting that $\hat{W}_{3i} \in I_3$ is equivalent to saying that $\hat{Z}_{3i} = \dfrac{\sqrt{n_3}\left( \bar{X}_{3i} - \hat{\mu}_0 \right)}{\hat{\sigma}_0} \in I_3^{**}$ (see Appendix B.2), where

$$I_3^{**} = \left[ -c_3 L_3 - w_1\sqrt{\frac{n_1}{n_3}} - z_2\sqrt{\frac{n_2}{n_3}}, c_3 L_3 - w_1\sqrt{\frac{n_1}{n_3}} - z_2\sqrt{\frac{n_2}{n_3}} \right].$$

Based on the above discussions, $\hat{P}_{a3}$ can be defined as

$$\hat{P}_{a3} = \int_{w_1 \in I_{12}} \int_{z_2 \in I_{22}^{**}} \Pr\left(\hat{Z}_{3i} \in I_3^{**}\right) f_{\hat{W}_{1i}}\left(w_1\right) f_{\hat{Z}_{2i}}\left(z_2\right) \mathrm{d}z_2 \mathrm{d}w_1 .$$

$$= \int_{w_1 \in I_{12}} \int_{z_2 \in I_{22}^{**}} \left[ \Phi\left( U\sqrt{\frac{n_3}{mn}} + V\left( c_3 L_3 - w_1\sqrt{\frac{n_1}{n_3}} - z_2\sqrt{\frac{n_2}{n_3}} \right) + \delta\sqrt{n_3} \right) - \Phi\left( U\sqrt{\frac{n_3}{mn}} - \right.\right.$$

$$\left.\left. -V\left( c_3 L_3 + w_1\sqrt{\frac{n_1}{n_3}} + z_2\sqrt{\frac{n_2}{n_3}} \right) + \delta\sqrt{n_3} \right) \right] f_{\hat{W}_{1i}}\left(w_1 \middle| \hat{\mu}_0, \hat{\sigma}_0\right) f_{\hat{Z}_{2i}}\left(z_2 \middle| \hat{\mu}_0, \hat{\sigma}_0\right) \mathrm{d}z_2 \mathrm{d}w_1, \qquad (21)$$

where the random variables $\hat{W}_{1i}$ and $\hat{Z}_{2i}$ are independent of one another. In Equation (21),

$$f_{\hat{Z}_{2i}}\left(z_2 \middle| \hat{\mu}_0, \hat{\sigma}_0\right) = V\phi\left( U\sqrt{\frac{n_2}{mn}} + Vz_2 + \delta\sqrt{n_2} \right) \qquad (22)$$

and $f_{\hat{W}_{1i}}\left(w_1 \middle| \hat{\mu}_0, \hat{\sigma}_0\right)$ is given in Equation (20). Appendix B.3 explains the derivation of $f_{\hat{Z}_{2i}}\left(z_2 \middle| \hat{\mu}_0, \hat{\sigma}_0\right)$.

The probability of taking the second sample is (Khoo et al. 2013)

$$\hat{P}_2 = \Pr\left(\hat{W}_{1i} \in I_{12} \middle| \hat{\mu}_0, \hat{\sigma}_0\right)$$

$$= \Phi\left( U\sqrt{\frac{n_1}{mn}} + VL_{12} + \delta\sqrt{n_1} \right) - \Phi\left( U\sqrt{\frac{n_1}{mn}} + VL_{11} + \delta\sqrt{n_1} \right) +$$

$$\Phi\left( U\sqrt{\frac{n_1}{mn}} - VL_{11} + \delta\sqrt{n_1} \right) - \Phi\left( U\sqrt{\frac{n_1}{mn}} - VL_{12} + \delta\sqrt{n_1} \right). \qquad (23)$$

Similarly, the probability of taking the third sample can be obtained as follows (see Appendix B.4):

$$\hat{P}_3 = \int_{w_1 \in I_{12}} \Pr\left(\hat{W}_{2i} \in I_{22} \middle| \hat{W}_{1i} = w_1, \hat{\mu}_0, \hat{\sigma}_0\right) f_{\hat{W}_{1i}}\left(w_1 \middle| \hat{\mu}_0, \hat{\sigma}_0\right) \mathrm{d}w_1$$

$$= \int_{w_1 \in I_{12}} \left[ \Phi\left( U\sqrt{\frac{n_2}{mn}} + V\left( c_2 L_{22} - w_1\sqrt{\frac{n_1}{n_2}} \right) + \delta\sqrt{n_2} \right) - \Phi\left( U\sqrt{\frac{n_2}{mn}} + V\left( c_2 L_{21} - w_1\sqrt{\frac{n_1}{n_2}} \right) \right.\right.$$

$$\left.\left. + \delta\sqrt{n_2} \right) \right] f_{\hat{W}_{1i}}\left( w_1 \middle| \hat{\mu}_0, \hat{\sigma}_0 \right) \mathrm{d}w_1 + \int_{w_1 \in I_{12}} \left[ \Phi\left( U\sqrt{\frac{n_2}{mn}} - V\left( c_2 L_{21} + w_1\sqrt{\frac{n_1}{n_2}} \right) + \delta\sqrt{n_2} \right) \right.$$

$$\left. - \Phi\left( U\sqrt{\frac{n_2}{mn}} - V\left( c_2 L_{22} + w_1\sqrt{\frac{n_1}{n_2}} \right) + \delta\sqrt{n_2} \right) \right] f_{\hat{W}_{1i}}\left( w_1 \middle| \hat{\mu}_0, \hat{\sigma}_0 \right) \mathrm{d}w_1. \qquad (24)$$

The ASS of the revised $\mathrm{TS}_E$ $\bar{X}$ chart at each sampling stage is

$$\mathrm{ASS} = \int_{-\infty}^{\infty} \int_{0}^{\infty} \left( n_1 + n_2\hat{P}_2 + n_3\hat{P}_3 \right) f_U(u)\, f_V(v)\, \mathrm{d}v\mathrm{d}u\,. \qquad (25)$$

Note that $f_U(u)$ and $f_V(v)$ in Equation (25) are given in Equations (17) and (18), respectively.

If process parameters are known, the ARL value of the revised $\mathrm{TS}_K$ $\bar{X}$ chart is a constant and hence, the standard deviation of the ARL is zero. However, when the target values of the process mean, $\mu_0$ and standard deviation, $\sigma_0$, are estimated, different Phase-I samples are used by different practitioners in the estimation. This results in different design parameters of the $\mathrm{TS}_E$ $\bar{X}$ chart, resulting in different values of ARL and standard deviation of the ARL (SDARL). Thus, the ARL of the estimated process parameters based $\mathrm{TS}_E$ $\bar{X}$ chart is a random variable and the average value of this performance measure can be calculated as the average of the ARLs (AARL), which is based on the ARL performances of the $\mathrm{TS}_E$ $\bar{X}$ chart averaged across different practitioners. In line with this phenomenon, in this paper, the AARL, as well as the SDARL criteria are used as the performance measures of the revised $\mathrm{TS}_E$ $\bar{X}$ chart. On similar lines, the average of the ANOS (AANOS) and standard deviation of the ANOS (SDANOS) will also be adopted as the performance measures of the $\mathrm{TS}_E$ $\bar{X}$ chart when process parameters are estimated.

The AARL and SDARL values are computed as

$$\mathrm{AARL} = \int_{-\infty}^{\infty} \int_{0}^{\infty} \left( \frac{1}{1-\hat{P}_a} \right) f_U(u) f_V(v)\, \mathrm{d}v\mathrm{d}u\,, \qquad (26)$$

and

$$\text{SDARL} = \left[\int_{-\infty}^{\infty}\int_{0}^{\infty}\left(\frac{1}{1-\hat{P}_a}\right)^2 f_U(u)f_V(v)\,\mathrm{d}v\mathrm{d}u - \text{AARL}^2\right]^{1/2}, \tag{27}$$

respectively, while the AANOS and SDANOS values are obtained as

$$\text{AANOS} = \int_{-\infty}^{\infty}\int_{0}^{\infty}\left(n_1 + n_2\hat{P}_2 + n_3\hat{P}_3\right)\left(\frac{1}{1-\hat{P}_a}\right) f_U(u)f_V(v)\,\mathrm{d}v\mathrm{d}u \tag{28}$$

and

$$\text{SDANOS} = \sqrt{\text{E}(\text{ANOS}^2) - (\text{AANOS})^2}, \tag{29}$$

respectively, where

$$\text{E}(\text{ANOS}^2) = \int_{-\infty}^{\infty}\int_{0}^{\infty}\left[\left(n_1 + n_2\hat{P}_2 + n_3\hat{P}_3\right)\left(\frac{1}{1-\hat{P}_a}\right)\right]^2 f_U(u)f_V(v)\,\mathrm{d}v\mathrm{d}u. \tag{30}$$

In this study, all integrals are solved numerically using the Legendre-Gauss quadrature method.

## 4. Optimal designs of the revised TS $\bar{X}$ charts

In this section, the optimal designs of the revised $\text{TS}_K$ $\bar{X}$ and revised $\text{TS}_E$ $\bar{X}$ charts in minimizing the values of (i) ANOS($\delta$) and (ii) ARL($\delta$), as well as (iii) AANOS($\delta$) and (iv) AARL($\delta$), respectively, are elaborated, where $\delta(>0)$ is the size of a standardized mean shift where a quick detection is needed. The optimal designs of the revised $\text{TS}_K$ $\bar{X}$ and revised $\text{TS}_E$ $\bar{X}$ charts mentioned below need to satisfy a specified in-control average sample size ($\text{ASS}_0$) criterion. Optimization programs are written in the MATLAB software to compute the optimal parameters of the revised $\text{TS}_K$ $\bar{X}$ and revised $\text{TS}_E$ $\bar{X}$ charts. These programs are provided in the supplementary materials.

### *4.1 Optimal designs of the revised $\text{TS}_K$ $\bar{X}$ chart*

In this section, the optimal designs of the revised $\text{TS}_K$ $\bar{X}$ chart in minimizing (i) ANOS($\delta$) and (ii) ARL($\delta$) values are elaborated. Since the ANOS criterion is preferred over the ARL criterion for adaptive sample size type charts, the step-by-step procedure in computing the optimal

parameters ($n_1$, $n_2$, $n_3$, $L_{11}$, $L_{12}$ $L_{21}$, $L_{22}$, $L_3$) of the revised $TS_K$ $\bar{X}$ chart in minimizing the ANOS($\delta$) value is discussed first in Section 4.1.1.

*4.1.1 Computation of optimal parameters in minimizing ANOS($\delta$)*

The optimization model of the revised $TS_K$ $\bar{X}$ chart in minimizing ANOS($\delta$) is presented as follows:

$$\underset{n_1,n_2,n_3,L_{11},L_{12},L_{21},L_{22},L_3}{\text{Minimize}} \quad \text{ANOS}(\delta) \tag{31a}$$

subject to the constraints

$$\text{ANOS}(0) = \tau_1 \tag{31b}$$

and

$$\text{ASS}_0 = n_0 . \tag{31c}$$

Note that ANOS(0) (for $\delta = 0$) and ANOS($\delta$) (for $\delta > 0$) are computed using Equation (10), while $\tau_1$ in Equation (31b) is the desired ANOS(0) value and $n_0$ is a specified value of $ASS_0$ which is usually set to be the same as the fixed sample size of the Shewhart $\bar{X}$ chart.

The step-by-step procedure in computing the optimal parameters ($n_1$, $n_2$, $n_3$, $L_{11}$, $L_{12}$ $L_{21}$, $L_{22}$, $L_3$) of the revised $TS_K$ $\bar{X}$ chart by minimizing the ANOS($\delta$) value for the shift size $\delta$ is given in Steps 1 to 11. Note that the intervals of the limits $L_{12}$, $L_{11}$ and $L_{22}$ (see Steps 4, 5 and 6, respectively) are chosen as it is found that these intervals are large enough to give the smallest ANOS($\delta$) value, based on the values of $\tau$ and $n_0$ considered.

Step 1. Specify the values of $\tau_1$, $n_0$ and $\delta$. In addition, initialize $ANOS_{min} = \infty$.

Step 2. Select a combination of sample sizes $(n_1, n_2, n_3)$, where $1 \leq n_1 \leq n_0 - 1$, $1 \leq n_2 \leq n_0$ and $1 \leq n_3 \leq 2n_0$ that satisfy the constraint $n_1 + n_2 + n_3 > n_0$ and go to Step 3. If no new $(n_1, n_2, n_3)$ combination is possible, go to Step 11.

Step 3. Initialize $L_{12}$ = 2.40, $L_{11}$ = 0.50 and $L_{22}$ = 2.50. Then proceed to Step 7.

Step 4. If 2.40 ≤ $L_{12}$ ≤ 5.50, increase $L_{12}$ by 0.01 and proceed to Step 7. Otherwise, return to Step 2.

Step 5. If 0.50 ≤ $L_{11}$ ≤1.70, increase $L_{11}$ by 0.01 and proceed to Step 7. Otherwise, reset $L_{11}$ = 0.65 and return to Step 4.

Step 6. If 2.50 ≤ $L_{22}$ ≤ 5.20, increase $L_{22}$ by 0.01 and proceed to Step 7. Otherwise, reset $L_{22}$ = 2.50 and return to Step 5.

Step 7. Compute $L_{21}$ that satisfies Equation (31c).

Step 8. Compute $L_3$ that satisfies Equation (31b).

Step 9. For the shift $\delta$ specified in Step 1, compute ANOS($\delta$) using Equation (10), based on the parameters ($n_1$, $n_2$, $n_3$, $L_{11}$, $L_{12}$ $L_{21}$, $L_{22}$, $L_3$) determined prior to Step 9.

Step 10. If ANOS($\delta$) < $\text{ANOS}_{\text{min}}$, then let $\text{ANOS}_{\text{min}}$ = ANOS($\delta$). Here, $\text{ANOS}_{\text{min}}$ records the smallest ANOS($\delta$) value that corresponds to the parameters ($n_1$, $n_2$, $n_3$, $L_{11}$, $L_{12}$ $L_{21}$, $L_{22}$, $L_3$). Return to Step 6.

Step 11. $\text{ANOS}_{\text{min}}$ gives the smallest ANOS($\delta$) value. The parameters ($n_1$, $n_2$, $n_3$, $L_{11}$, $L_{12}$ $L_{21}$, $L_{22}$, $L_3$) that produce this $\text{ANOS}_{\text{min}}$ value are the optimal parameters of the revised $\text{TS}_K$ $\bar{X}$ chart that minimize the ANOS($\delta$) value for the shift size $\delta$.

Figure 2 provides a flowchart that summarizes the above 11 steps optimization procedure of the revised $\text{TS}_K$ $\bar{X}$ chart in minimizing the ANOS($\delta$) value.

Insert Figure 2 here

For illustration, $\tau_1$ = 370, $n_0$ ∈ {5, 7} and $\delta$ ∈ {0.1, 0.2, 0.3, 0.5, 0.7, 1, 1.5, 2} are considered. Table 3 presents the values of the optimal parameters ($n_1$, $n_2$, $n_3$, $L_{11}$, $L_{12}$ $L_{21}$, $L_{22}$, $L_3$) and the corresponding ANOS($\delta$) values of the revised $\text{TS}_K$ $\bar{X}$ chart for the $n_0$ and $\delta$ values considered. For example, when $n_0$ = 7 and $\delta$ = 1, the optimal parameters ($n_1$, $n_2$, $n_3$, $L_{11}$, $L_{12}$ $L_{21}$, $L_{22}$, $L_3$) = (6, 3, 3, 1.34, 2.61, 0.2064, 2.61, 2.5337) produce the smallest ANOS(1) (=

9.99) value among all parameter combinations that give ANOS(0) = $\tau_1$ (= 370). Table 3 also gives the ANOS($\delta$) values for the optimal known process parameters based double sampling $\bar{X}$ (denoted as $\text{DS}_K$ $\bar{X}$) chart which will be used in the discussion in Section 5.

Insert Table 3 here

*4.1.2 Computation of optimal parameters in minimizing ARL($\delta$)*

The optimization model of the revised $\text{TS}_K$ $\bar{X}$ chart in minimizing ARL($\delta$) is presented as follows:

$$\underset{n_1,n_2,n_3,L_{11},L_{12},L_{21},L_{22},L_3}{\text{Minimize}} \quad \text{ARL}(\delta) \tag{32a}$$

subject to the constraints

$$\text{ARL}(0) = \tau_2 \tag{32b}$$

and

$$\text{ASS}_0 = n_0 . \tag{32c}$$

Note that $\tau_2$ in Equation (32b) is the desired value of ARL(0). To compute the optimal parameters of the $\text{TS}_K$ $\bar{X}$ chart in minimizing the ARL($\delta$) value, a similar approach to that of Steps 1 – 11 in Section 4.1.1 is employed. The only differences are (i) $\text{ANOS}_{\text{min}}$ and ANOS($\delta$) in the aforementioned procedure in Section 4.1.1 are replaced by $\text{ARL}_{\text{min}}$ and ARL($\delta$), respectively, and (ii) Equations (31c), (31b) and (10) in Steps 7, 8 and 9 of the aforementioned procedure are replaced by Equations (32c), (32b) and (9), respectively.

Table 4 presents the values of the optimal parameters ($n_1$, $n_2$, $n_3$, $L_{11}$, $L_{12}$ $L_{21}$, $L_{22}$, $L_3$) in minimizing the ARL($\delta$) value of the revised $\text{TS}_K$ $\bar{X}$ chart for $\tau_2$ = 370 and the same $n_0$ and $\delta$ values considered in Section 4.1.1. For example, when $n_0$ = 7 and $\delta$ = 1, the optimal parameters ($n_1$, $n_2$, $n_3$, $L_{11}$, $L_{12}$ $L_{21}$, $L_{22}$, $L_3$) = (5, 5, 12, 1.11, 5.14, 1.7626, 4.77, 2.8000) produce the

smallest ARL(1) (= 1.21) value, among all parameter combinations that give the value ARL(0) = $\tau_2$ (= 370).

Insert Table 4 here

### 4.2 Optimal designs of the revised $TS_E$ $\bar{X}$ chart

The optimal designs of the revised $TS_E$ $\bar{X}$ chart in minimizing the (i) AANOS($\delta$) and (ii) AARL($\delta$) ($\delta > 0$) values are discussed in this section when the process parameters $\mu_0$ and $\sigma_0$ of the revised TS $\bar{X}$ chart are estimated from the in-control Phase-I samples.

#### *4.2.1 Computation of optimal parameters in minimizing AANOS($\delta$)*

The optimization model of the revised $TS_E$ $\bar{X}$ chart in minimizing AANOS($\delta$) is given as follows:

$$\underset{n_1,n_2,n_3,L_{11},L_{12},L_{21},L_{22},L_3}{\text{Minimize}} \quad \text{AANOS}(\delta) \tag{33a}$$

subject to the constraints

$$\text{AANOS}(0) = \tau_3 \tag{33b}$$

and

$$\text{ASS}_0 = n_0. \tag{33c}$$

Note that $\tau_3$ in Equation (33b) is the desired value of AANOS(0), where the latter is computed using Equation (28) by letting $\delta = 0$.

The step-by-step procedure in Section 4.1.1 can also be used to compute the optimal parameters ($n_1$, $n_2$, $n_3$, $L_{11}$, $L_{12}$ $L_{21}$, $L_{22}$, $L_3$) of the revised $TS_E$ $\bar{X}$ chart, except that an additional input parameter *m* (number of in-control Phase-I samples) needs to be specified in Step 1 of the procedure together with the other input parameters $\tau_3$, $n_0$ and $\delta$. In addition, $ANOS_{min}$ and ANOS($\delta$) in the procedure are replaced by $AANOS_{min}$ and AANOS($\delta$),

respectively. Note that Equations (31c), (31b) and (10) are replaced by Equations (33c), (33b) and (28), respectively, in Steps 7, 8 and 9 of the aforementioned procedure. Table 5 provides the optimal parameters $(n_1, n_2, n_3, L_{11}, L_{12}\ L_{21}, L_{22}, L_3)$ of the revised $\text{TS}_E$ $\bar{X}$ chart that minimizes the $\text{AANOS}(\delta)$ value for the shift size $\delta$, when $m \in \{20, 40, 80\}$, $\delta \in \{0.1, 0.2, 0.3, 0.5, 0.7, 1, 1.5, 2\}$, $n_0 \in \{5, 7\}$ and $\tau_3 = 370$. The $\text{AANOS}(\delta)$ and $\text{SDANOS}(\delta)$ values computed using the optimal parameters in Table 5 are given in Table 6. For illustration, consider $\delta = 1$, $n_0 = 5$ and $m = 20$. For this case, the optimal parameters $(n_1, n_2, n_3, L_{11}, L_{12}\ L_{21}, L_{22}, L_3) = (4, 3, 3, 1.09, 2.88, 1.8424, 2.72, 2.5852)$ of the revised $\text{TS}_E$ $\bar{X}$ chart are obtained (see Table 5) and using these optimal parameters result in the smallest AANOS(1) (= 10.63) value and the corresponding $\text{SDANOS}(1)$ value is 2.60 (see Table 6). Table 6 also provides the $\text{AANOS}(\delta)$ and $\text{SDANOS}(\delta)$ values for the optimal $\text{DS}_E$ $\bar{X}$ chart.

Insert Table 5 here

Insert Table 6 here

*4.2.2 Computation of optimal parameters in minimizing AARL($\delta$)*

The optimization model for the revised $\text{TS}_E$ $\bar{X}$ chart in minimizing the $\text{AARL}(\delta)$ value is given as follows:

$$\underset{n_1, n_2, n_3, L_{11}, L_{12}, L_{21}, L_{22}, L_3}{\text{Minimize}} \quad \text{AARL}(\delta) \tag{34a}$$

subject to the constraints

$$\text{AARL}(0) = \tau_4 \tag{34b}$$

and

$$\text{ASS}_0 = n_0. \tag{34c}$$

The $\tau_4$ in Equation (34b) is the desired value of AARL(0), where the latter is computed using Equation (26) by letting $\delta = 0$.

The optimization model in (34a) – (34c) is employed to obtain the optimal parameters $(n_1, n_2, n_3, L_{11}, L_{12}\ L_{21}, L_{22}, L_3)$ of the revised $\text{TS}_E$ $\bar{X}$ chart in minimizing the $\text{AARL}(\delta)$ value. The 11 steps optimal design procedure mentioned in Section 4.1.1 can be used in minimizing the $\text{AARL}(\delta)$ value but by substituting $\text{ANOS}_{\text{min}}$ and $\text{ANOS}(\delta)$ with $\text{AARL}_{\text{min}}$ and $\text{AARL}(\delta)$, respectively. Note that Equations (31c), (31b) and (10) are replaced by Equations (34c), (34b) and (26), respectively, in Steps 7, 8 and 9 of the aforementioned procedure.

Table 7 provides the optimal parameters $(n_1, n_2, n_3, L_{11}, L_{12}\ L_{21}, L_{22}, L_3)$ of the revised $\text{TS}_E$ $\bar{X}$ chart that minimizes the $\text{AARL}(\delta)$ value for fixed values of $\delta$, $m$ and $n_0$ when $\tau_4 = 370$. The $\text{AARL}(\delta)$ and $\text{SDARL}(\delta)$ values computed using the optimal parameters in Table 7 are given in Table 8. For illustration, for the case $\delta = 0.5$, $n_0 = 5$ and $m = 20$, the optimal parameters $(n_1, n_2, n_3, L_{11}, L_{12}\ L_{21}, L_{22}, L_3)$ = (3, 5, 10, 1.16, 4.83, 1.5825, 4.87, 2.8190) are obtained for the revised $\text{TS}_E$ $\bar{X}$ chart (see Table 7) and using these optimal parameters result in the smallest AARL(1) value of 10.76 and the corresponding $\text{SDARL}(1)$ value of 11.90 (see Table 8). Table 8 also provides the $\text{AARL}(\delta)$ and $\text{SDARL}(\delta)$ values for the optimal $\text{DS}_E$ $\bar{X}$ chart.

Insert Table 7 here

Insert Table 8 here

## 5. Performance analyses

In this section, the performances of the optimal revised $\text{TS}_K$ $\bar{X}$ and optimal revised $\text{TS}_E$ $\bar{X}$ charts when process parameters are known and estimated, respectively, are investigated. When process parameters are known, the optimal revised $\text{TS}_K$ $\bar{X}$ chart is compared with the optimal $\text{DS}_K$ $\bar{X}$ chart of Daudin (1992), in terms of the ANOS($\delta$) and ARL($\delta$) criteria in Tables 3 and 4, respectively. In addition, the optimal revised $\text{TS}_K$ $\bar{X}$ chart is compared with the $\text{AS}_2$ $\bar{X}$ and $\text{AS}_3$ $\bar{X}$ charts of Prabhu et al. (1993), and Zimmer, Montgomery and Runger (1998), respectively, in terms of the ARL($\delta$) criterion in Table 4. In the case when process parameters are estimated,

the optimal revised $TS_E$ $\bar{X}$ chart is compared with the optimal $DS_E$ $\bar{X}$ chart of Khoo et al. (2013), in terms of the AANOS($\delta$) and SDANOS($\delta$) criteria in Table 6, while a comparison between these two charts using the AARL($\delta$) and SDARL($\delta$) criteria is given in Table 8. The speed in which the revised TS $\bar{X}$ chart is quicker (or slower) in detecting a process mean shift compared with an existing chart at hand is measured in terms of percentage. The results presented in this paper have been verified with simulations.

The results in Table 3 show that the revised $TS_K$ $\bar{X}$ chart outperforms the $DS_K$ $\bar{X}$ chart for small and moderate shifts ($\delta \leq 1$), in terms of ANOS. For instance, when $n_0 = 5$, ANOS(0.7) = 18.50 for the revised $TS_K$ $\bar{X}$ chart is significantly lower than that of the $DS_K$ $\bar{X}$ chart (ANOS(0.7) = 25.48), which indicates that the revised $TS_K$ $\bar{X}$ chart is 27.39% quicker than the $DS_K$ $\bar{X}$ chart in detecting a shift of size $\delta = 0.7$. However, for large shifts ($\delta = 1.5$ and 2), the $DS_K$ $\bar{X}$ chart performs slightly better than the revised $TS_K$ $\bar{X}$ chart but the difference is negligible. For example, when $n_0 = 5$, ANOS (1.5) = 5.34 and 5.33 for the revised $TS_K$ $\bar{X}$ and $DS_K$ $\bar{X}$ charts, respectively, where the difference is negligible, i.e. the $DS_K$ $\bar{X}$ chart is 0.19% faster than the revised $TS_K$ $\bar{X}$ chart in detecting the shift of size $\delta = 1.5$. In terms of the ARL criterion, the revised $TS_K$ $\bar{X}$ chart is found to be superior to the $DS_K$ $\bar{X}$ chart in detecting shifts but the two charts have equal performances in the detection of a large shift, say $\delta = 2$ (see Table 4). For example, when $n_0 = 5$, ARL(0.7) = 2.84 and 3.60 for the revised $TS_K$ $\bar{X}$ and $DS_K$ $\bar{X}$ charts, respectively (see Table 4), which indicates that the revised $TS_K$ $\bar{X}$ chart is 21.11% quicker than the $DS_K$ $\bar{X}$ chart in detecting a shift of size $\delta = 0.7$. However, for $\delta = 2$, both charts have the same value of ARL(2) = 1.

In comparison with the $AS_3$ $\bar{X}$ chart, the revised $TS_K$ $\bar{X}$ chart prevails in detecting all shift sizes in terms of the ARL($\delta$) criterion. For example, when $n_0 = 5$, ARL(0.7) = 2.84 for the revised $TS_K$ $\bar{X}$ chart is significantly lower than that for the $AS_3$ $\bar{X}$ chart whose ARL(0.7) = 6.17

(see Table 4). In terms of the percentage of improvement, the revised $TS_K$ $\bar{X}$ chart is 53.97% quicker than the $AS_3$ $\bar{X}$ chart in detecting the shift $\delta = 0.7$.

A comparison between the revised $TS_K$ $\bar{X}$ and $AS_2$ $\bar{X}$ charts shows that the former has lower ARL($\delta$) value than the latter for all shift sizes. For example, when $n_0 = 5$, ARL(0.5) = 7.04 for the revised $TS_K$ $\bar{X}$ chart is significantly lower than that of the $AS_2$ $\bar{X}$ chart (ARL(0.5) = 18.30), which indicates that the revised $TS_K$ $\bar{X}$ chart is 61.53% quicker than the $AS_2$ $\bar{X}$ chart in detecting a shift of size $\delta = 0.5$ (see Table 4).

Table 6 shows a comparison of the AANOS($\delta$) and SDANOS($\delta$) values between the revised $TS_E$ $\bar{X}$ and $DS_E$ $\bar{X}$ charts, for $m \in \{20, 40, 80, \infty\}$. It is obvious in Table 6 that the revised $TS_E$ $\bar{X}$ chart outperforms the $DS_E$ $\bar{X}$ chart, in terms of the SDANOS($\delta$) criterion, for almost all shift sizes $\delta$, when the process parameters are estimated. This is because the revised $TS_E$ $\bar{X}$ chart has a lower SDANOS($\delta$) value than the $DS_E$ $\bar{X}$ chart, for the same value of $\delta$. For example, when $m = 20$, $n_0 = 5$ and $\delta \in \{0.1, 0.2, 0.3, 0.5, 0.7, 1, 1.5, 2\}$, SDANOS($\delta$) $\in$ {189.42, 145.93, 83.05, 19.56, 7.49, 2.60, 0.68, 0.30} and {202.44, 154.76, 91.80, 22.91, 6.99, 3.04, 0.90, 0.46} for the revised $TS_E$ $\bar{X}$ and $DS_E$ $\bar{X}$ charts, respectively, where almost all the SDANOS($\delta$) values of the former are lower than that of the latter. When comparison is made in terms of the AANOS($\delta$) criterion, it is found that the revised $TS_E$ $\bar{X}$ chart prevails over the $DS_E$ $\bar{X}$ chart for $0.1 \leq \delta \leq 1$. For instance, consider $m = 20$ and $n_0 = 5$. For this case, AANOS($\delta$) $\in$ {308.79, 191.78, 105.17, 38.84, 20.74, 10.63} and {314.22, 204.11, 116.54, 42.46, 22.29, 11.36} for the revised $TS_E$ $\bar{X}$ and $DS_E$ $\bar{X}$ charts, respectively, when $\delta \in \{0.1, 0.2, 0.3, 0.5, 0.7, 1\}$, where the former has lower AANOS($\delta$) values than the latter. In this example, the revised $TS_E$ $\bar{X}$ chart is 6.95% quicker than the $DS_E$ $\bar{X}$ chart in detecting a shift of size $\delta = 0.7$. The decrease in the AANOS($\delta$) values vary from 1.73% to 9.76% when the $TS_E$ $\bar{X}$ chart is used in place of the $DS_E$ $\bar{X}$ chart, based on $m = 20$, $n_0 = 5$ and $0.1 \leq \delta \leq 1$ (see Table 6). For $\delta > 1$, the $TS_E$ $\bar{X}$ chart is

slightly slower than the $DS_E$ $\bar{X}$ chart in detecting process shifts. For example, when $\delta = 1.5$, $n_0 = 5$ and $m = 20$, AANOS(1.5) = 5.45 and 5.42 for the revised $TS_E$ $\bar{X}$ and $DS_E$ $\bar{X}$ charts, respectively, where the former is 0.55% slower than the latter in detecting the shift $\delta = 1.5$.

Another important trend noticeable in Table 6 is that as $m$ increases, the AANOS($\delta$) values of both the revised $TS_E$ $\bar{X}$ and $DS_E$ $\bar{X}$ charts converge to the ANOS($\delta$) values of their known process parameters counterparts in Table 3. As an example, when $n_0 = 5$, $\delta = 0.1$ and $m \in \{20, 40, 80\}$, AANOS(0.1) $\in \{308.79, 291.05, 276.49\}$ and $\{314.22, 300.32, 289.06\}$ for the revised $TS_E$ $\bar{X}$ and $DS_E$ $\bar{X}$ charts, respectively, where these values converge to the respective ANOS(0.1) values of the corresponding revised $TS_K$ $\bar{X}$ (= 253.41) and $DS_K$ $\bar{X}$ (= 270.17) charts in Table 3, as $m$ increases. It is also observed in Table 6 that the $\mathrm{AANOS}(\delta)$ and $\mathrm{SDANOS}(\delta)$ performances of the revised $TS_E$ $\bar{X}$ and $DS_E$ $\bar{X}$ charts improve as $n_0$ increases. For example, for the revised $TS_E$ $\bar{X}$ chart, when $m = 40$, $\big(\mathrm{AANOS}(0.2), \mathrm{SDANOS}(0.2)\big)$ = (164.16, 88.12) for $n_0 = 5$ and these values decrease to $\big(\mathrm{AANOS}(0.2), \mathrm{SDANOS}(0.2)\big)$ = (143.83, 65.76) as $n_0$ increases to 7. Similarly, for the $DS_E$ $\bar{X}$ chart, for the same $m$ and $\delta$ combination, the $\big(\mathrm{AANOS}(0.2), \mathrm{SDANOS}(0.2)\big)$ values decrease from (180.09, 94.79) to (157.24, 70.38) as $n_0$ increases from 5 to 7.

The $\mathrm{AANOS}(\delta)$ and $\mathrm{SDANOS}(\delta)$ values in Table 6 for the revised $TS_E$ $\bar{X}$ and $DS_E$ $\bar{X}$ charts change as the number of the Phase-I samples, $m$ changes, even though $n_0$ remains constant. For instance, when $n_0 = 5$, $\big(\mathrm{AANOS}(0.3), \mathrm{SDANOS}(0.3)\big) \in \{(105.17, 83.05), (88.33, 49.91), (80.36, 24.97)\}$, for the revised $TS_E$ $\bar{X}$ chart, when $m \in \{20, 40, 80\}$, where it is seen that the $\mathrm{AANOS}(0.3)$ and $\mathrm{SDANOS}(0.3)$ values vary with $m$ for a fixed value of $n_0$. Therefore, the $\mathrm{AANOS}(\delta)$ and $\mathrm{SDANOS}(\delta)$ values are random variables and their values depend on $m$. According to Jones and Steiner (2012); Gandy and Kvaløy (2013) and Zhang, Megahed, and Woodall (2014), the $\mathrm{SDANOS}(0)$ value of the estimated process parameters based chart should

be at most 10% of the $\mathrm{ANOS}(0)$ value of the chart's known process parameters counterpart so that the former performs satisfactorily even though there is still some considerable difference between the $\mathrm{AANOS}(0)$ value of the former and the $\mathrm{ANOS}(0)$ value of the latter.

Table 9 gives the $\mathrm{AANOS}(0)$ and $\mathrm{SDANOS}(0)$ values of the revised $\mathrm{TS}_E$ $\bar{X}$ chart for $m \in \{50, 100, 150, \ldots, 800, \infty\}$, computed using the optimal parameters of the revised $\mathrm{TS}_K$ $\bar{X}$ chart in minimizing ANOS(1.5), when $n_0 \in \{5, 7\}$ and ANOS(0) $\in \{200, 370\}$. The aforementioned optimal parameters computed when ANOS(0) = 200 are $(n_1, n_2, n_3, L_{11}, L_{12}\ L_{21}, L_{22}, L_3) \in \{(4, 2, 2, 0.95, 2.43, 1.0734, 2.50, 2.6518), (5, 3, 4, 0.94, 2.35, 0.5237, 2.6785)\}$ for $n_0 \in \{5, 7\}$, while those adopted from Table 3 when ANOS(0) = 370 are $(n_1, n_2, n_3, L_{11}, L_{12}\ L_{21}, L_{22}, L_3) = \{(4, 2, 2, 0.71, 2.65, 2.0490, 2.76, 2.7871)$ and $(5, 3, 8, 1.21, 2.47, 0.6710, 2.60, 3.4207)\}$ for $n_0 \in \{5, 7\}$. For example, by adopting these optimal parameters on the revised $\mathrm{TS}_E$ $\bar{X}$ chart give $\mathrm{AANOS}(0) = 199.73$ and $\mathrm{SDANOS}(0) = 19.27$ for $n_0 = 5$ and $m = 550$ when the process is in-control.

Insert Table 9 here

An analysis of Table 8 shows that when a comparison is made between the revised $\mathrm{TS}_E$ $\bar{X}$ and $\mathrm{DS}_E$ $\bar{X}$ charts, in terms of the AARL($\delta$) criterion, the former surpasses the latter for all shift sizes $\delta$, as the former has a lower AARL($\delta$) value than the latter for the same value of $\delta$. For example, when $m = 20$ and $n_0 = 5$, AARL($\delta$) $\in \{290.18, 149.22, 60.44, 10.76, 3.51, 1.56, 1.06, 1.00\}$ and $\{296.24, 163.14, 72.37, 14.74, 4.72, 1.83, 1.09, 1.00\}$ for $\delta \in \{0.1, 0.2, 0.3, 0.5, 0.7, 1, 1.5, 2\}$, for the $\mathrm{TS}_E$ $\bar{X}$ and $\mathrm{DS}_E$ $\bar{X}$ charts, respectively. However, in terms of the SDARL($\delta$) criterion, the $\mathrm{TS}_E$ $\bar{X}$ chart outperforms the $\mathrm{DS}_E$ $\bar{X}$ chart for all values of $\delta$ and $m$ when $n_0 = 5$ but when $n_0 = 7$, the $\mathrm{TS}_E$ $\bar{X}$ chart is superior to the $\mathrm{DS}_E$ $\bar{X}$ chart only for smaller values of $\delta$ and $m$.

Table 10 gives the AARL(0) and SDARL(0) values of the revised $TS_E$ $\bar{X}$ chart, for $m \in \{50, 150, 250, \ldots, 750, 800, \ldots, 1150, \infty\}$, computed using the optimal parameters of the revised $TS_K$ $\bar{X}$ chart in minimizing AARL(1.5), based on $n_0 \in \{5, 7\}$ and ARL(0) $\in \{200, 370\}$. The optimal parameters computed for the revised $TS_K$ $\bar{X}$ chart when ARL(0) = 200 are $(n_1, n_2, n_3, L_{11}, L_{12}\ L_{21}, L_{22}, L_3) \in \{(4, 2, 5, 1.06, 4.79, 1.6369, 4.45, 2.7015), (6, 3, 5, 1.19, 4.44, 1.7979, 4.45\ 2.7183)\}$ for $n_0 \in \{5, 7\}$, while those adopted from Table 4 when ARL(0) = 370 are $(n_1, n_2, n_3, L_{11}, L_{12}\ L_{21}, L_{22}, L_3)$ = {(3, 3, 7, 0.74, 4.94, 1.6076, 4.58, 2.8820) and (5, 4, 10, 0.91, 3.38, 1.8386, 3.4, 3.0284)} for $n_0 \in \{5, 7\}$. For example, by adopting these optimal parameters on the revised $TS_E$ $\bar{X}$ chart give AARL(0) = 198.70 and SDARL(0) = 19.96 for $n_0$ = 5 and *m* = 800 when the process is in-control (see Table 10).

By investigating Tables 9 and 10, it is seen that the SDANOS(0) and SDARL(0) values of the revised $TS_E$ $\bar{X}$ chart decrease as *m* increases. For $m \geq 550$ (see Table 9) and $m \geq 800$ (see Table 10) when $n_0$ = 5, the SDANOS(0) and SDARL(0) values, respectively, become smaller than 10% of the corresponding ANOS(0) and ARL(0) (= 200) values of the $TS_K$ $\bar{X}$ chart. The value of *m* for any (ANOS(0), $n_0$) or (ARL(0), $n_0$) combination corresponding to the boldfaced SDANOS(0) (in Table 9) or SDARL(0) (in Table 10) value, respectively, represent the minimum number of in-control Phase-I samples needed so that the SDANOS(0) or SDARL(0) value is smaller than 10% of the corresponding ANOS(0) or ARL(0) value, respectively. This value of *m* will ensure that the AANOS(0) and AARL(0) values of the revised $TS_E$ $\bar{X}$ chart are considerably close to the respective ANOS(0) and ARL(0) values of the revised $TS_K$ $\bar{X}$ chart.

Insert Table 10 here

## 6. An implementation of the revised $TS_E$ $\bar{X}$ chart

This section illustrates the implementation of the revised $TS_E$ $\bar{X}$ chart in a real application using a dataset of the flow width measurements (in microns) for the hard bake process adopted from

Montgomery (2009). The Phase-I data which comprise $m$ = 20 samples, each having $n$ = 5 observations are used to estimate the in-control process mean $\hat{\mu}_0$ and standard deviation $\hat{\sigma}_0$ using Equations (11) and (12), respectively. The estimates are $\hat{\mu}_0$ = 1.493 microns and $\hat{\sigma}_0$ = 0.152 microns. Suppose that the revised $TS_E$ $\bar{X}$ chart is optimally designed in minimizing AANOS(1), i.e. to enable a quick detection of the shift size $\delta$ = 1, based on AANOS(0) = 370, $m$ = 20 and $n_0$ = 5. Consequently, the optimal parameters are obtained from Table 5 as $(n_1, n_2, n_3, L_{11}, L_{12}, L_{21}, L_{22}, L_3)$ = (4, 3, 3, 1.09, 2.88, 1.8424, 2.72, 2.5852). These optimal parameters are used in the Phase-II process monitoring. Figure 3 provides a flowchart to explain the operation of the revised $TS_E$ $\bar{X}$ chart in the Phase-II process by using the values of the aforementioned optimal parameters.

Insert Figure 3 here

The dataset for the Phase-II analysis which contains 14 sampling stages, where $n_1$ = 4, $n_2$ = 3 and $n_3$ = 3, and the computed control charting statistics of the revised $TS_E$ $\bar{X}$ chart are given in Table 11. The control charting statistics, $\hat{W}_{1i}$, $\hat{W}_{2i}$ and $\hat{W}_{3i}$, for these 14 sampling stages in Phase-II are plotted in Figure 4. The working of the chart is elaborated as follows: At sampling stage 1 ($i$ = 1), a sample of size $n_1$ = 4 is taken at inspection level 1, where $\bar{X}_{1i}$ = 1.4696 and $\hat{W}_{11}$ = –0.3079 are computed. As $\hat{W}_{11} \in I_{11}$ = [–1.09, 1.09], sampling stage 1 is in-control. Then at sampling stage 2 ($i$ = 2), a sample of size $n_1$ = 4 is taken at inspection level 1, which gives $\hat{W}_{12}$ = 1.5303 $\in I_{12}$ = [–2.88, –1.09) $\cup$ (1.09, 2.88], hence, a second sample of size $n_2$ = 3 is taken at inspection level 2 of the same sampling stage. Consequently, $\bar{X}_{22}$ = 1.4240, $Y_{22}$ = 1.5299 and $\hat{W}_{22}$ = 0.6423 are computed. As $\hat{W}_{22} \in I_{21}$ = [–1.8424, 1.8424], sampling stage 2 is in-control. At sampling stage 3 ($i$ = 3), a sample of size $n_1$ = 4 is taken at inspection level 1,

that gives $\hat{W}_{13} = 0.5816 \in I_{11} = [-1.09, 1.09]$, hence, sampling stage 3 is in-control. Subsequently, at sampling stage 4 ($i = 4$), a sample of size $n_1 = 4$ is taken at inspection level 1, which gives $\hat{W}_{14} = -1.3895 \in I_{12} = [-2.88, -1.09) \cup (1.09, 2.88]$. Then, a second sample of size $n_2 = 3$ is taken at inspection level 2 of sampling stage 4, which gives $\hat{W}_{24} = -1.0618 \in I_{21} = [-1.8424, 1.8424]$, i.e. sampling stage 4 is in-control.

Insert Table 11 here

Insert Figure 4 here

The same procedure of taking samples and computing the charting statistics is continued until sampling stage 14 ($i = 14$). At sampling stage 14, a sample of size $n_1 = 4$ is taken at inspection level 1 and $\hat{W}_{1(14)} = 1.7079$ is computed. As $\hat{W}_{1(14)} \in I_{12} = [-2.88, -1.09) \cup (1.09, 2.88]$, a second sample of size $n_2 = 3$ is taken at inspection level 2 of the same sampling stage. Then, $\hat{W}_{2(14)} = 2.5204 \in I_{22} = [-2.72, -1.8424) \cup (1.8424, 2.72]$ is obtained, hence, a third sample of size $n_3 = 3$ is taken at inspection level 3 of the same sampling stage. It follows that $\bar{X}_{3(14)} = 1.6399$, $Y_{3(14)} = 1.6384$ and $\hat{W}_{3(14)} = 3.0250$ are computed. As $\hat{W}_{3(14)}$ $(= 3.0250) \notin I_3 = [-2.5852, 2.5852]$, an out-of-control is signaled at sampling stage 14 (see Figure 2). Following this out-of-control signal, corrective actions should be taken to remove the assignable cause(s) so that the out-of-control condition becomes in-control again.

## 7. Conclusions

In this research, we provide corrections to address the oversight in the formulae derivation for computing the run length performance of the known process parameters based TS $\bar{X}$ chart in He, Grigoryan, and Sigh (2002). To assess the efficiency of the revised $\text{TS}_K$ $\bar{X}$ chart, performance comparisons with the existing $\text{DS}_K$ $\bar{X}$, $\text{AS}_2$ $\bar{X}$ and $\text{AS}_3$ $\bar{X}$ charts, in terms of the

ANOS and ARL criteria are made. In addition, the revised TS $\bar{X}$ chart based on estimated process parameters (called revised $\mathrm{TS}_E$ $\bar{X}$ chart) is also proposed. The efficiency of the revised $\mathrm{TS}_E$ $\bar{X}$ chart is measured using the AANOS (AARL) and SDANOS(SDARL) criteria and is compared with the $\mathrm{DS}_E$ $\bar{X}$ chart. The numerical analyses performed in Section 5 show that the revised $\mathrm{TS}_K$ $\bar{X}$ and revised $\mathrm{TS}_E$ $\bar{X}$ charts outperform the $\mathrm{DS}_K$ $\bar{X}$ and $\mathrm{DS}_E$ $\bar{X}$ charts, respectively, in the detection of most sizes of shifts in the process mean. Tables of optimal parameters of the revised $\mathrm{TS}_K$ $\bar{X}$, as well as revised $\mathrm{TS}_E$ $\bar{X}$ charts in minimizing the out-of-control ANOS and ARL, as well as AANOS and AARL values, respectively, for selected combinations of input parameters are given.

The quality of a production process or a product being manufactured is affected by, for example, deviations from the nominal value of the (i) weight of raw materials, (ii) process temperature, (iii) viscosity of a certain chemical, (iv) process humidity and (v) machine setting. The revised $\mathrm{TS}_K$ $\bar{X}$ and revised $\mathrm{TS}_E$ $\bar{X}$ charts are designed to detect these deviations quickly. These revised TS $\bar{X}$ charts can be applied in various production systems, such as in monitoring the stability of a plastic film process, monitoring the diameter of gears in an automobile industry and monitoring the pH level of a process that produces medicine in a pharmaceutical industry, to name some. Information obtained from the revised TS $\bar{X}$ charts in process monitoring of production systems will help decision makers in taking suitable corrective actions, in order to reduce process deviations for quality enhancement.

The effects of the estimation of process parameters from the in-control Phase-I dataset on the in-control and out-of-control performances of the revised $\mathrm{TS}_E$ $\bar{X}$ chart are investigated. It is found that the revised $\mathrm{TS}_E$ $\bar{X}$ chart adopting the optimal parameters of its known process parameters counterpart requires a very large number of the in-control Phase-I samples in order to have a closer performance to the latter. It is shown that the out-of-control AANOS (AARL) performance of the revised $\mathrm{TS}_E$ $\bar{X}$ chart is poorer than the out-of-control ANOS (ARL)

performance of the revised $TS_K$ $\bar{X}$ chart. A table listing the minimum required number of in-control Phase-I samples so that the in-control SDANOS(SDARL) value of the revised $TS_E$ $\bar{X}$ chart is at most 10% of the corresponding in-control ANOS(ARL) value of the revised $TS_K$ $\bar{X}$ chart is presented.

This research focuses on the univariate TS $\bar{X}$ chart with known and estimated process parameters. The development of a multivariate triple sampling $T^2$ chart with known and estimated process parameters can be explored in the future as many real-life situations involve multivariate data. Future researches can be conducted to enhance the shift detection speed of the revised TS $\bar{X}$ chart by incorporating the auxiliary information concept, as well as considering the variable sampling interval feature. Furthermore, the TS technique can be integrated into Shewhart charts for the process variability, such as the *R*, *S* and $S^2$ charts.

**Acknowledgement**

This research was supported by the Universiti Sains Malaysia, Research University grant, number 1001.PMATHS.8011039.

**References**

Abbasi, S., and A. Haq. 2019. "Enhanced adaptive CUSUM charts for process mean." *Journal of Statistical Computation and Simulation* 89 (13), 2562-2582.

Aparisi, F., E. Epprecht, A. Carrión, and O. Ruiz. 2014. "The variable sample size variable dimension $T^2$ control chart." *International Journal of Production Research* 52 (2), 368-383.

Aparisi, F., J. Mosquera, and E. K. Epprecht. 2018. "Simultaneously guaranteeing the in-control and out-of-control performances of the $S^2$ control chart with estimated variance." *Quality and Reliability Engineering International* 34 (6), 1110-1126.

Carot, V., J. M. Jabaloyes, and T. Carot. 2002. "Combined double sampling and variable sampling interval $\bar{X}$ chart." *International Journal of Production Research* 40 (9), 2175-2186.

Castagliola, P., P. C. Oprime, and M. B. C. Khoo. 2017. "The double sampling $S^2$ chart with estimated process variance." *Communications in Statistics-Theory and Methods* 46 (7), 3556-3573.

Celano, G., and S. Chakraborti. 2020. "A distribution-free Shewhart-type Mann–Whitney control chart for monitoring finite horizon productions." *International Journal of Production Research*, doi.org/10.1080/00207543.2020.1802079.

Costa, A. F. B. 1994. "$\bar{X}$ charts with variable sample size." *Journal of Quality Technology 26* (3), 155-163.

Costa, A. F. B. 1999. "$\bar{X}$ charts with variable parameters." *Journal of Quality Technology 31* (4), 408-416.

Costa, A. F. B. 2017. "The double sampling range chart." *Quality and Reliability Engineering International* 33 (8), 2739-2745.

Croasdale, R. 1974. "Control charts for a double-sampling scheme based on average production run lengths." *International Journal of Production Research* 12 (5), 585-592.

Daudin, J. J. 1992. "Double sampling $\bar{X}$ charts." *Journal of Quality Technology* 24 (2), 78-87.

De la Torre Gutiérrez, H., and D.T. Pham. 2018. "Identification of patterns in control charts for processes with statistically correlated noise." *International Journal of Production Research* 56 (4), 1504-1520.

Faraz, A., C. Heuchenne, and E. Saniga. 2018. "An exact method for designing Shewhart and $S^2$ control charts to guarantee in-control performance." *International Journal of Production Research* 56 (7), 2570-2584.

Faraz, A., W. H. Woodall, and C. Heuchenne. 2015. “Guaranteed conditional performance of the $S^2$ control chart with estimated parameters.” *International Journal of Production Research* 53 (14), 4405-4413.

Gandy, A., and J. T. Kvaløy. 2013. “Guaranteed conditional performance of control charts via bootstrap methods.” *Scandinavian Journal of Statistics* 40 (4), 647-668.

Guo, B., and B. X. Wang. 2016. “The variable sampling interval $S^2$ chart with known or unknown in-control variance.” *International Journal of Production Research* 54 (11), 3365-3379.

Haq, A., and M. B. C. Khoo. 2018. “A new double sampling control chart for monitoring process mean using auxiliary information.” *Journal of Statistical Computation and Simulation* 88 (5), 869-899.

Haridy, S., M. Shamsuzzaman, I. Alsyouf, and A. Mukherjee. 2020. “An improved design of exponentially weighted moving average scheme for monitoring attributes.” *International Journal of Production Research* 58 (3), 931-946.

He, D., A. Grigoryan, and M. Sigh. 2002. “Design of double- and triple-sampling $\bar{X}$ control charts using genetic algorithms.” *International Journal of Production Research* 40 (6), 1387-1404.

Hou, S., and K. Yu. 2021. “A non-parametric CUSUM control chart for process distribution change detection and change type diagnosis.” *International Journal of Production Research* 59 (4), 1166-1186.

Hsu, L. F. 2004. “Note on ‘Design of double-and triple-sampling $\bar{X}$ control charts using genetic algorithms’.” *International Journal of Production Research* 42 (5), 1043-1047.

Hu, X., and P. Castagliola. 2019. “A re-evaluation of the run rules $\bar{X}$ chart when the process parameters are unknown.” *Quality Technology & Quantitative Management* 16 (6), 696-725.

Hu, X., P. Castagliola, Y. Ma, and W. Huang. 2018. "Guaranteed in-control performance of the synthetic chart with estimated parameters." *Quality and Reliability Engineering International* 34 (5), 759-771.

Huang, S., J. Yang, and M. Xie. 2020. "A double-sampling SPM scheme for simultaneously monitoring of location and scale shifts and its joint design with maintenance strategies." *Journal of Manufacturing Systems* 54, 94-102.

Irianto, D., and N. Shinozaki. 1998. "An optimal double sampling $\bar{X}$ control chart." *International Journal of Industrial Engineering - Applications and Practice* 5 (3), 226-234.

Khoo, M. B. C., E. K. Tan, Z. L. Chong, and S. Haridy. 2015. "Side-sensitive group runs double sampling (SSGRDS) chart for detecting mean shifts." *International Journal of Production Research* 53 (15), 4735-4753.

Khoo, M. B. C., H. C. Lee, Z. Wu, C. H. Chen, and P. Castagliola. 2010. A synthetic double sampling control chart for the process mean. *IIE Transactions*, 43 (1), 23-38.

Khoo, M. B. C., W. L. Teoh, P. Castagliola, and M. H. Lee. 2013. "Optimal designs of the double sampling $\bar{X}$ chart with estimated parameters. *International Journal of Production Economics* 144 (1), 345-357.

Krupskii, P., F. Harrou, A. S. Hering, and Y. Sun. 2020. "Copula-based monitoring schemes for non-Gaussian multivariate processes." *Journal of Quality Technology* 52 (3), 219-234.

Lee, M. H., and M. B. C. Khoo. 2019. "Double sampling np chart with estimated process parameter." *Communications in Statistics - Simulation and Computation* doi.org/10.1080/03610918.2019.1599017.

Li, C., D. Wang, and F. Zhu. 2019. "Detecting mean increases in zero truncated INAR (1) processes." *International Journal of Production Research* 57 (17), 5589-5603.

Montgomery, D. C. 2009. *Introduction to Statistical Quality Control*, 6th ed. New York: John Wiley & Sons, Inc.

Motsepa, C. M., J. C. Malela-Majika, P. Castagliola, and S. C. Shongwe. 2020. "A side-sensitive double sampling $\bar{X}$ monitoring scheme with estimated process parameters." *Communications in Statistics - Simulation and Computation* doi.org/10.1080/03610918.2020.1722835.

Prabhu, S. S., G. C. Runger, and J. B. Keats. 1993. "$\bar{X}$ chart with adaptive sample sizes." *International Journal of Production Research* 31 (12), 2895-2909.

Qu, L., M. B. C. Khoo, P. Castagliola, and Z. He. 2018a. "Exponential cumulative sums chart for detecting shifts in time-between-events." *International Journal of Production Research* 56 (10), 3683-3698.

Qu, L., S. He, M. B. C. Khoo, and P. Castagliola. 2018b. "A CUSUM chart for detecting the intensity ratio of negative events." *International Journal of Production Research 56*(19), 6553-6567.

Reynolds, M. R. Jr., R. W., Amin, J. C. Arnold, and J. A. Nachlas. 1988. "Charts with variable sampling intervals." *Technometrics* 30 (2), 181-192.

Saha, S., M. B. C. Khoo, M. H. Lee, and P. Castagliola. 2018. "A side-sensitive modified group runs double sampling (SSMGRDS) control chart for detecting mean shifts." *Communications in Statistics - Simulation and Computation* 47 (5), 1353-1369.

Saha, S., M. B. C. Khoo, P. S. Ng, and Z. L. Chong. 2019. "Variable sampling interval run sum median charts with known and estimated process parameters." *Computers & Industrial Engineering*, 127, 571-587.

Stankus, S. E., and K. K. Castillo-Villar. 2019. "An Improved multivariate generalised likelihood ratio control chart for the monitoring of point clouds from 3D laser scanners." *International Journal of Production Research* 57 (8), 2344-2355.

Wang, K., and F. Tsung. 2020. "Bayesian cross-product quality control via transfer learning." *International Journal of Production Research* doi.org/10.1080/00207543.2020.1845413.

You, H. W., M. B. C. Khoo, M. H. Lee, and P. Castagliola. 2015. "Synthetic double sampling $\bar{X}$ chart with estimated process parameters." *Quality Technology & Quantitative Management* 12 (4), 579-604.

Zhang, M., F. M. Megahed, and W. H. Woodall. 2014. "Exponential CUSUM charts with estimated control limits." *Quality and Reliability Engineering International* 30 (2), 275-286.

Zimmer, L. S., D. C. Montgomery, and G. C. Runger. 1998. "Evaluation of a three-state adaptive sample size $\bar{X}$ control chart." *International Journal of Production Research* 36 (3), 733-743.

## Appendix A

This appendix explains the mathematical derivations to show that $W_{1i} \in I_{12}$, $W_{2i} \in I_{22}$ and $W_{3i} \in I_3$ are equivalent to $Z'_{1i} \in I^*_{12}$, $Z'_{2i} \in I^*_{22}$ and $Z'_{3i} \in I^*_3$, respectively. These derivations are given in Appendices A1, A2, and A3, respectively. Furthermore, the formula derivation of $P_3$ in Equation (8) is explained in Appendix A4. The notations defined in Section 3.1 are

$r_2 = \sqrt{n_1 + n_2}$, $c_2 = \sqrt{\dfrac{n_1 + n_2}{n_2}}$, $r_3 = \sqrt{n_1 + n_2 + n_3}$, $c_3 = \sqrt{\dfrac{n_1 + n_2 + n_3}{n_3}}$,

$Z'_{1i} = \sqrt{n_1}\left(\bar{X}_{1i} - \mu_0 + \delta\sigma_0\right)/\sigma_0$, $Z'_{2i} = \sqrt{n_2}\left(\bar{X}_{2i} - \mu_0 + \delta\sigma_0\right)/\sigma_0$ and

$Z'_{3i} = \sqrt{n_3}\left(\bar{X}_{3i} - \mu_0 + \delta\sigma_0\right)/\sigma_0$. $Z'_{1i}$, $Z'_{2i}$ and $Z'_{3i}$ are standard normal random variables from their definitions.

### A1. Mathematical derivation to show that $W_{1i} \in I_{12}$ is equivalent to $Z'_{1i} \in I^*_{12}$

$$\Pr\left(W_{1i} \in I_{12}\right) = \Pr\left(-L_{12} \le W_{1i} \le -L_{11}\right) + \Pr\left(L_{11} \le W_{1i} \le L_{12}\right).$$

$$\text{But } \Pr\left(-L_{12} \le W_{1i} \le -L_{11}\right) = \Pr\left(-L_{12} \le \frac{\left(\bar{X}_{1i} - \mu_0\right)\sqrt{n_1}}{\sigma_0} \le -L_{11}\right)$$

$$= \Pr\left(-\frac{L_{12}\sigma_0}{\sqrt{n_1}} \le \bar{X}_{1i} - \mu_0 \le -\frac{L_{11}\sigma_0}{\sqrt{n_1}}\right)$$

$$= \Pr\left(-\frac{L_{12}\sigma_0\sqrt{n_1}}{\sigma_0\sqrt{n_1}} \le \frac{\sqrt{n_1}\left(\bar{X}_{1i} - \mu_0 + \delta\sigma_0\right)}{\sigma_0} - \frac{\delta\sigma_0\sqrt{n_1}}{\sigma_0} \le -\frac{L_{11}\sigma_0\sqrt{n_1}}{\sigma_0\sqrt{n_1}}\right)$$

$$= \Pr\left(-L_{12} \le \frac{\left(\bar{X}_{1i} - \mu_0 + \delta\sigma_0\right)\sqrt{n_1}}{\sigma_0} - \delta\sqrt{n_1} \le -L_{11}\right)$$

$$= \Pr\left(-L_{12} + \delta\sqrt{n_1} \le Z'_{1i} \le -L_{11} + \delta\sqrt{n_1}\right).$$

Similarly, it can be shown that

$$\Pr\left(L_{11} \le W_{1i} \le L_{12}\right) = \Pr\left(L_{11} + \delta\sqrt{n_1} \le Z'_{1i} \le L_{12} + \delta\sqrt{n_1}\right).$$

Therefore,

$$\Pr\left(W_{1i} \in I_{12}\right) = \Pr\left(-L_{12} + \delta\sqrt{n_1} \le Z'_{1i} \le -L_{11} + \delta\sqrt{n_1}\right) +$$

$$\Pr\left(L_{11} + \delta\sqrt{n_1} \le Z'_{1i} \le L_{12} + \delta\sqrt{n_1}\right) \qquad \text{(A1)}$$

From Equation (A1), it is clear that $W_{1i} \in I_{12}$ is equivalent to $Z'_{1i} \in I^*_{12}$, where

$$I^*_{12} = \left[-L_{12} + \delta\sqrt{n_1}, -L_{11} + \delta\sqrt{n_1}\right] \cup \left[L_{11} + \delta\sqrt{n_1}, L_{12} + \delta\sqrt{n_1}\right]. \qquad \text{(A2)}$$

**A2. Mathematical derivation to show that $W_{2i} \in I_{22}$ is equivalent to $Z'_{2i} \in I^*_{22}$**

$$\Pr\left(W_{2i} \in I_{22}\right) = \Pr\left(-L_{22} \le W_{2i} \le -L_{21}\right) + \Pr\left(L_{21} \le W_{2i} \le L_{22}\right).$$

$$\text{But } \Pr\left(-L_{22} \le W_{2i} \le -L_{21}\right) = \Pr\left(-L_{22} \le \frac{\left(Y_{2i} - \mu_0\right)\sqrt{n_1 + n_2}}{\sigma_0} \le -L_{21}\right)$$

$$= \Pr\left(-\frac{L_{22}\sigma_0}{\sqrt{n_1 + n_2}} \le \frac{n_1\bar{X}_{1i} + n_2\bar{X}_{2i}}{n_1 + n_2} - \mu_0 \le -\frac{L_{21}\sigma_0}{\sqrt{n_1 + n_2}}\right)$$

$$= \Pr\left( -\frac{L_{22}\sigma_0}{r_2\sigma_0} \le \frac{n_1\left(\bar{X}_{1i} - \mu_0 + \delta\sigma_0\right) + n_2\left(\bar{X}_{2i} - \mu_0 + \delta\sigma_0\right)}{\left(n_1 + n_2\right)\sigma_0} - \frac{\delta\sigma_0}{\sigma_0} \le -\frac{L_{21}\sigma_0}{r_2\sigma_0} \right)$$

$$= \Pr\left( -\frac{L_{22}\left(n_1 + n_2\right)}{r_2} \le Z'_{1i}\sqrt{n_1} + Z'_{2i}\sqrt{n_2} - \delta\left(n_1 + n_2\right) \le -\frac{L_{21}\left(n_1 + n_2\right)}{r_2} \right)$$

$$= \Pr\left( -c_2L_{22} + r_2c_2\delta - Z'_{1i}\sqrt{\frac{n_1}{n_2}} \le Z'_{2i} \le -c_2L_{21} + r_2c_2\delta - Z'_{1i}\sqrt{\frac{n_1}{n_2}} \right).$$

Similarly, it can be shown that

$$\Pr\left(L_{21} \le W_{2i} \le L_{22}\right) = \Pr\left( c_2L_{21} + r_2c_2\delta - Z'_{1i}\sqrt{\frac{n_1}{n_2}} \le Z'_{2i} \le c_2L_{22} + r_2c_2\delta - Z'_{1i}\sqrt{\frac{n_1}{n_2}} \right).$$

Therefore,

$$\Pr\left(W_{2i} \in I_{22}\right) = \Pr\left( -c_2L_{22} + r_2c_2\delta - Z'_{1i}\sqrt{\frac{n_1}{n_2}} \le Z'_{2i} \le -c_2L_{21} + r_2c_2\delta - Z'_{1i}\sqrt{\frac{n_1}{n_2}} \right) +$$

$$\Pr\left( c_2L_{21} + r_2c_2\delta - Z'_{1i}\sqrt{\frac{n_1}{n_2}} \le Z'_{2i} \le c_2L_{22} + r_2c_2\delta - Z'_{1i}\sqrt{\frac{n_1}{n_2}} \right). \quad \text{(A3)}$$

From Equation (A3), it is clear that $W_{2i} \in I_{22}$ is equivalent to $Z'_{2i} \in I^*_{22}$, where

$$I^*_{22} = \left[ -c_2L_{22} + r_2c_2\delta - z'_1\sqrt{\frac{n_1}{n_2}}, -c_2L_{21} + r_2c_2\delta - z'_1\sqrt{\frac{n_1}{n_2}} \right] \cup$$

$$\left[ c_2L_{21} + r_2c_2\delta - z'_1\sqrt{\frac{n_1}{n_2}}, c_2L_{22} + r_2c_2\delta - z'_1\sqrt{\frac{n_1}{n_2}} \right]. \quad \text{(A4)}$$

**A3. Mathematical derivation to show that $W_{3i} \in I_3$ is equivalent to $Z'_{3i} \in I^*_3$**

$$\Pr\left(W_{3i} \in I_3\right) = \Pr\left(-L_3 \le W_{3i} \le L_3\right)$$

$$= \Pr\left( -L_3 \le \frac{\left(Y_{3i} - \mu_0\right)\sqrt{n_1 + n_2 + n_3}}{\sigma_0} \le L_3 \right)$$

$$= \Pr\left( -\frac{L_3\sigma_0}{r_3} \le \frac{n_1\bar{X}_{1i} + n_2\bar{X}_{2i} + n_3\bar{X}_{3i}}{n_1+n_2+n_3} - \mu_0 \le \frac{L_3\sigma_0}{r_3} \right)$$

$$= \Pr\left( \frac{-L_3\sigma_0}{\sigma_0 r_3} < \frac{n_1\left(\bar{X}_{1i} - \mu_0 + \delta\sigma_0\right) + n_2\left(\bar{X}_{2i} - \mu_0 + \delta\sigma_0\right) + n_3\left(\bar{X}_{3i} - \mu_0 + \delta\sigma_0\right)}{\left(n_1+n_2+n_3\right)\sigma_0} - \frac{\delta\sigma_0}{\sigma_0} \le \frac{L_3\sigma_0}{\sigma_0 r_3} \right)$$

$$= \Pr\left( -\frac{L_3}{r_3} \le \frac{\sqrt{n_1}Z'_{1i}}{\left(n_1+n_2+n_3\right)} + \frac{\sqrt{n_2}Z'_{2i}}{\left(n_1+n_2+n_3\right)} + \frac{\sqrt{n_3}Z'_{3i}}{\left(n_1+n_2+n_3\right)} - \delta \le \frac{L_3}{r_3} \right)$$

$$= \Pr\left( -r_3L_3 + \delta\left(n_1+n_2+n_3\right) - \sqrt{n_1}Z'_{1i} - \sqrt{n_2}Z'_{2i} \le \sqrt{n_3}Z'_{3i} \le r_3L_3 + \delta\left(n_1+n_2+n_3\right) - \sqrt{n_1}Z'_{1i} - \sqrt{n_2}Z'_{2i} \right)$$

$$= \Pr\left( -c_3L_3 + r_3c_3\delta - Z'_{1i}\sqrt{\frac{n_1}{n_3}} - Z'_{2i}\sqrt{\frac{n_2}{n_3}} \le Z'_{3i} \le c_3L_3 + r_3c_3\delta - Z'_{1i}\sqrt{\frac{n_1}{n_3}} - Z'_{2i}\sqrt{\frac{n_2}{n_3}} \right). \tag{A5}$$

From Equation (A5), it is clear that $W_{3i} \in I_3$ is equivalent to $Z'_{3i} \in I_3^*$, where

$$I_3^* = \left[ -c_3L_3 + r_3c_3\delta - z'_1\sqrt{\frac{n_1}{n_3}} - z'_2\sqrt{\frac{n_2}{n_3}}, c_3L_3 + r_3c_3\delta - z'_1\sqrt{\frac{n_1}{n_3}} - z'_2\sqrt{\frac{n_2}{n_3}} \right]. \tag{A6}$$

## A4. Formulae derivation of $P_3$ in Equation (8)

In Section 3.1, it is known that

$$P_3 = \Pr\left(W_{2i} \in I_{22} \middle| W_{1i} \in I_{12}\right) = \int_{w_1 \in I_{12}} \Pr\left(W_{2i} \in I_{22} \middle| W_{1i} = w_1\right) f_{W_{1i}}\left(w_1\right) \mathrm{d}w_1. \tag{A7}$$

$P_3$ in Equation (A7) involves $W_{2i} \in I_{22}$ and $W_{1i} \in I_{12}$. The probabilities, $\Pr\left(W_{1i} \in I_{12}\right)$ and $\Pr\left(W_{2i} \in I_{22}\right)$ are given in Equations (A1) and (A3), respectively. By incorporating the results in Equations (A1) and (A3) into Equation (A7) gives

$$P_3 = \int_{z_1' \in I_{12}^*} \left[ \Phi\left( -c_2 L_{21} + r_2 c_2 \delta - z_1' \sqrt{\frac{n_1}{n_2}} \right) - \Phi\left( -c_2 L_{22} + r_2 c_2 \delta - z_1' \sqrt{\frac{n_1}{n_2}} \right) \right] \phi(z_1') \, \mathrm{d}z_1' +$$

$$\int_{z_1' \in I_{12}^*} \left[ \Phi\left( c_2 L_{22} + r_2 c_2 \delta - z_1' \sqrt{\frac{n_1}{n_2}} \right) - \Phi\left( c_2 L_{21} + r_2 c_2 \delta - z_1' \sqrt{\frac{n_1}{n_2}} \right) \right] \phi(z_1') \, \mathrm{d}z_1', \qquad \text{(A8)}$$

where $I_{12}^*$ is given in Equation (A2).

## Appendix B

This appendix explains the mathematical derivations to show that $\hat{W}_{2i} \in I_{22}$ and $\hat{W}_{3i} \in I_3$ are equivalent to $\hat{Z}_{2i} \in I_{22}^{**}$ and $\hat{Z}_{3i} \in I_3^{**}$, respectively. These derivations are given in Appendices B1 and B2, respectively. In addition, the formulae derivations of $f_{\hat{Z}_{2i}}\left(z_2 \middle| \hat{\mu}_0, \hat{\sigma}_0\right)$ and $\hat{P}_3$ in Equations (22) and (24), respectively, are explained in Appendices B3 and B4. The notations defined in Section 3.2 are $\hat{W}_{1i} = \dfrac{\sqrt{n_1}\left(\bar{X}_{1i} - \hat{\mu}_0\right)}{\hat{\sigma}_0}$, $\hat{Z}_{2i} = \dfrac{\sqrt{n_2}\left(\bar{X}_{2i} - \hat{\mu}_0\right)}{\hat{\sigma}_0}$ and $\hat{Z}_{3i} = \dfrac{\sqrt{n_3}\left(\bar{X}_{3i} - \hat{\mu}_0\right)}{\hat{\sigma}_0}$. $\hat{W}_{1i}$, $\hat{Z}_{2i}$ and $\hat{Z}_{3i}$ are standard normal random variables from their definitions.

### B1. Mathematical derivation to show that $\hat{W}_{2i} \in I_{22}$ is equivalent to $\hat{Z}_{2i} \in I_{22}^{**}$

$$\Pr\left(\hat{W}_{2i} \in I_{22}\right) = \Pr\left(-L_{22} \le \hat{W}_{2i} \le -L_{21}\right) + \Pr\left(L_{21} \le \hat{W}_{2i} \le L_{22}\right).$$

But $\Pr\left(-L_{22} \le \hat{W}_{2i} \le -L_{21}\right) = \Pr\left( -L_{22} \le \dfrac{\left(Y_{2i} - \hat{\mu}_0\right)\sqrt{n_1 + n_2}}{\hat{\sigma}_0} \le -L_{21} \right)$

$$= \Pr\left( -\frac{L_{22}\hat{\sigma}_0}{\sqrt{n_1 + n_2}} \le \frac{n_1 \bar{X}_{1i} + n_2 \bar{X}_{2i}}{n_1 + n_2} - \hat{\mu}_0 \le -\frac{L_{21}\hat{\sigma}_0}{\sqrt{n_1 + n_2}} \right)$$

$$= \Pr\left( -L_{22}\sqrt{n_1+n_2} \le \frac{n_1\left(\bar{X}_{1i}-\hat{\mu}_0\right)}{\hat{\sigma}_0} + \frac{n_2\left(\bar{X}_{2i}-\hat{\mu}_0\right)}{\hat{\sigma}_0} \le -L_{21}\sqrt{n_1+n_2} \right)$$

$$= \Pr\left( -L_{22}\sqrt{\frac{n_1+n_2}{n_2}} - \hat{W}_{1i}\sqrt{\frac{n_1}{n_2}} \le \hat{Z}_{2i} \le -L_{21}\sqrt{\frac{n_1+n_2}{n_2}} - \hat{W}_{1i}\sqrt{\frac{n_1}{n_2}} \right)$$

$$= \Pr\left( -c_2 L_{22} - \hat{W}_{1i}\sqrt{\frac{n_1}{n_2}} \le \hat{Z}_{2i} \le -c_2 L_{21} - \hat{W}_{1i}\sqrt{\frac{n_1}{n_2}} \right).$$

Similarly, it can be shown that

$$\Pr\left( L_{21} \le \hat{W}_{2i} \le L_{22} \right) = \Pr\left( c_2 L_{21} - \hat{W}_{1i}\sqrt{\frac{n_1}{n_2}} \le \hat{Z}_{2i} \le c_2 L_{22} - \hat{W}_{1i}\sqrt{\frac{n_1}{n_2}} \right).$$

Therefore,

$$\Pr\left( \hat{W}_{2i} \in I_{22} \right) = \Pr\left( -c_2 L_{22} - \hat{W}_{1i}\sqrt{\frac{n_1}{n_2}} \le \hat{Z}_{2i} \le -c_2 L_{21} - \hat{W}_{1i}\sqrt{\frac{n_1}{n_2}} \right) +$$

$$\Pr\left( c_2 L_{21} - \hat{W}_{1i}\sqrt{\frac{n_1}{n_2}} \le \hat{Z}_{2i} \le c_2 L_{22} - \hat{W}_{1i}\sqrt{\frac{n_1}{n_2}} \right). \qquad \text{(B1)}$$

From Equation (B1), it is clear that $\hat{W}_{2i} \in I_{22}$ is equivalent to $\hat{Z}_{2i} \in I_{22}^{**}$, where

$$I_{22}^{**} = \left[ -c_2 L_{22} - w_1\sqrt{\frac{n_1}{n_2}},\ -c_2 L_{21} - w_1\sqrt{\frac{n_1}{n_2}} \right] \cup \left[ c_2 L_{21} - w_1\sqrt{\frac{n_1}{n_2}},\ c_2 L_{22} - w_1\sqrt{\frac{n_1}{n_2}} \right]. \qquad \text{(B2)}$$

Note that $c_2$ is defined in Appendix A.

## B2. Mathematical derivation to show that $\hat{W}_{3i} \in I_3$ is equivalent to $\hat{Z}_{3i} \in I_3^{**}$

$$\Pr\left( \hat{W}_{3i} \in I_3 \right) = \Pr\left( -L_3 \le \hat{W}_{3i} \le L_3 \right)$$

$$= \Pr\left( -L_3 \le \frac{\left(Y_{3i}-\hat{\mu}_0\right)\sqrt{n_1+n_2+n_3}}{\hat{\sigma}_0} \le L_3 \right)$$

$$= \Pr\left( -\frac{L_3\hat{\sigma}_0}{r_3} \le \frac{n_1\bar{X}_{1i} + n_2\bar{X}_{2i} + n_3\bar{X}_{3i}}{n_1+n_2+n_3} - \hat{\mu}_0 \le \frac{L_3\hat{\sigma}_0}{r_3} \right)$$

$$= \Pr\left( \frac{-L_3\hat{\sigma}_0\left(n_1+n_2+n_3\right)}{\hat{\sigma}_0 r_3} \le \frac{n_1\left(\bar{X}_{1i}-\hat{\mu}_0\right)}{\hat{\sigma}_0} + \frac{n_2\left(\bar{X}_{2i}-\hat{\mu}_0\right)}{\hat{\sigma}_0} + \frac{n_3\left(\bar{X}_{3i}-\hat{\mu}_0\right)}{\hat{\sigma}_0} \le \frac{L_3\hat{\sigma}_0\left(n_1+n_2+n_3\right)}{\hat{\sigma}_0 r_3} \right)$$

$$= \Pr\left( -L_3 r_3 - \hat{W}_{1i}\sqrt{n_1} - \hat{Z}_{2i}\sqrt{n_2} \le \frac{n_3\left(\bar{X}_{3i}-\hat{\mu}_0\right)}{\hat{\sigma}_0} \le L_3 r_3 - \hat{W}_{1i}\sqrt{n_1} - \hat{Z}_{2i}\sqrt{n_2} \right).$$

$$= \Pr\left( \frac{-L_3 r_3}{\sqrt{n_3}} - \hat{W}_{1i}\sqrt{\frac{n_1}{n_3}} - \hat{Z}_{2i}\sqrt{\frac{n_2}{n_3}} \le \frac{\sqrt{n_3}\left(\bar{X}_{3i}-\hat{\mu}_0\right)}{\hat{\sigma}_0} \le \frac{L_3 r_3}{\sqrt{n_3}} - \hat{W}_{1i}\sqrt{\frac{n_1}{n_3}} - \hat{Z}_{2i}\sqrt{\frac{n_2}{n_3}} \right). \quad \text{(B3)}$$

From Equation (B3), it is clear that $\hat{W}_{3i} \in I_3$ is equivalent to $\hat{Z}_{3i} \in I_3^{**}$, where

$$I_3^{**} = \left[ -c_3 L_3 - w_1\sqrt{\frac{n_1}{n_3}} - z_2\sqrt{\frac{n_2}{n_3}}, c_3 L_3 - w_1\sqrt{\frac{n_1}{n_3}} - z_2\sqrt{\frac{n_2}{n_3}} \right]. \quad \text{(B4)}$$

From Equation (B4), we have

$$\Pr\left(\hat{W}_{3i} \in I_3\right)$$

$$= \Pr\left( \hat{\mu}_0 - \frac{\left(L_3 r_3 + \hat{W}_{1i}\sqrt{n_1} + \hat{Z}_{2i}\sqrt{n_2}\right)\hat{\sigma}_0}{n_3} \le \bar{X}_{3i} \le \hat{\mu}_0 + \frac{\left(L_3 r_3 - \hat{W}_{1i}\sqrt{n_1} - \hat{Z}_{2i}\sqrt{n_2}\right)\hat{\sigma}_0}{n_3} \right). \quad \text{(B5)}$$

As $\bar{X}_{3i} \sim N\left(\mu_0 - \delta\sigma_0, \frac{\sigma_0^2}{n_3}\right)$, Equation (B5) becomes

$$\Pr\left(\hat{W}_{3i} \in I_3\right)$$

$$= \Pr\left( \left(\hat{\mu}_0 - \mu_0\right)\frac{\sqrt{n_3}}{\sigma_0} - \frac{\hat{\sigma}_0}{\sigma_0}\left( c_3 L_3 + \hat{W}_{1i}\sqrt{\frac{n_1}{n_3}} + \hat{Z}_{2i}\sqrt{\frac{n_2}{n_3}} \right) + \delta\sqrt{n_3} \le \frac{\left(\bar{X}_{3i} - \mu_0 + \delta\sigma_0\right)\sqrt{n_3}}{\sigma_0} \le \right.$$

$$\left. \left(\hat{\mu}_0 - \mu_0\right)\frac{\sqrt{n_3}}{\sigma_0} + \frac{\hat{\sigma}_0}{\sigma_0}\left( c_3 L_3 - \hat{W}_{1i}\sqrt{\frac{n_1}{n_3}} - \hat{Z}_{2i}\sqrt{\frac{n_2}{n_3}} \right) + \delta\sqrt{n_3} \right)$$

$$= \Phi\left( U\sqrt{\frac{n_3}{mn}} + V\left( c_3 L_3 - \hat{W}_{1i}\sqrt{\frac{n_1}{n_3}} - \hat{Z}_{2i}\sqrt{\frac{n_2}{n_3}} \right) + \delta\sqrt{n_3} \right)$$

$$- \Phi\left( U\sqrt{\frac{n_3}{mn}} - V\left( c_3 L_3 + \hat{W}_{1i}\sqrt{\frac{n_1}{n_3}} + \hat{Z}_{2i}\sqrt{\frac{n_2}{n_3}} \right) + \delta\sqrt{n_3} \right). \quad \text{(B6)}$$

Note that $r_3$ and $c_3$ have been defined in Appendix A.

## B3. Formulae derivation of $f_{\hat{Z}_{2i}}(z_2|\hat{\mu}_0, \hat{\sigma}_0)$ in Equation (22)

From definition, $\hat{Z}_{2i} = \dfrac{\left(\bar{X}_{2i} - \hat{\mu}_0\right)\sqrt{n_2}}{\hat{\sigma}_0}$, where $\bar{X}_{2i} = \dfrac{\sum_{j=1}^{n_2} X_{2i,j}}{n_2}$ and $X_{2i,j} \sim N\left(\mu_0 - \delta\sigma_0, \sigma_0^2\right)$.

Let $F_{\hat{Z}_{2i}}\left(z_2|\hat{\mu}_0, \hat{\sigma}_0\right)$ be the conditional distribution function of $\hat{Z}_{2i}$, given $\hat{\mu}_0$ and $\hat{\sigma}_0$. Then

$$F_{\hat{Z}_{2i}}\left(z_2|\hat{\mu}_0, \hat{\sigma}_0\right) = \Pr\left(\hat{Z}_{2i} \le z_2 \middle| \hat{\mu}_0, \hat{\sigma}_0\right)$$

$$= \Pr\left( \bar{X}_{2i} \le \hat{\mu}_0 + \frac{\hat{\sigma}_0}{\sqrt{n_2}} z_2 \right). \quad \text{(B7)}$$

As $\bar{X}_{2i} \sim N\left(\mu_0 - \delta\sigma_0, \dfrac{\sigma_0^2}{n_2}\right)$, then Equation (B7) becomes

$$F_{\hat{Z}_{2i}}\left(z_2|\hat{\mu}_0, \hat{\sigma}_0\right) = \Phi\left( \left(\hat{\mu}_0 - \mu_0\right)\frac{\sqrt{n_2}}{\sigma_0} + \frac{\hat{\sigma}_0}{\sigma_0} z_2 + \delta\sqrt{n_2} \right).$$

$$= \Phi\left( U\sqrt{\frac{n_2}{mn}} + V z_2 + \delta\sqrt{n_2} \right), \quad \text{(B8)}$$

where $U = \left(\hat{\mu}_0 - \mu_0\right)\dfrac{\sqrt{mn}}{\sigma_0}$ and $V = \dfrac{\hat{\sigma}_0}{\sigma_0}$ (see Equations (15) and (16), respectively). The pdf of $\hat{Z}_{2i}$ $\left(\text{i.e.} f_{\hat{Z}_{2i}}\left(z_2|\hat{\mu}_0, \hat{\sigma}_0\right)\right)$ is obtained as the derivative of $F_{\hat{Z}_{2i}}\left(z_2|\hat{\mu}_0, \hat{\sigma}_0\right)$ in Equation (B8) with respect to $z_2$, i.e.

$$f_{\hat{Z}_{2i}}\left(z_2\left|\hat{\mu}_0,\hat{\sigma}_0\right.\right)=V\phi\left(U\sqrt{\frac{n_2}{mn}}+Vz_2+\delta\sqrt{n_2}\right). \tag{B9}$$

## B4. Formulae derivation of $\hat{P}_3$ in Equation (24)

In Section 3.2,

$$\hat{P}_3=\int_{w_1\in I_{12}}\Pr\left(\hat{W}_{2i}\in I_{22}\left|\hat{W}_{1i}=w_1,\hat{\mu}_0,\hat{\sigma}_0\right.\right)f_{\hat{W}_{1i}}\left(w_1\left|\hat{\mu}_0,\hat{\sigma}_0\right.\right)dw_1. \tag{B10}$$

$\hat{P}_3$ in Equation (B10) involves $\hat{W}_{1i}\in I_{12}$ and $\hat{W}_{2i}\in I_{22}$. From Figure 1,

$$\Pr\left(\hat{W}_{2i}\in I_{22}\right)=\Pr\left(-L_{22}\le\hat{W}_{2i}\le-L_{21}\right)+\Pr\left(L_{21}\le\hat{W}_{2i}\le L_{22}\right). \tag{B11}$$

In Equation (B11) (see Appendix B1),

$$\Pr\left(-L_{22}\le\hat{W}_{2i}\le-L_{21}\right)$$

$$=\Pr\left(\hat{\mu}_0-\frac{\left(L_{22}\sqrt{n_1+n_2}+\hat{W}_{1i}\sqrt{n_1}\right)\hat{\sigma}_0}{n_2}\le\bar{X}_{2i}\le\hat{\mu}_0-\frac{\left(L_{21}\sqrt{n_1+n_2}+\hat{W}_{1i}\sqrt{n_1}\right)\hat{\sigma}_0}{n_2}\right).$$

As $\bar{X}_{2i}\sim N\left(\mu_0-\delta\sigma_0,\frac{\sigma_0^2}{n_2}\right)$, then

$$\Pr\left(-L_{22}\le\hat{W}_{2i}\le-L_{21}\right)$$

$$=\Pr\left(\frac{\left(\hat{\mu}_0-\mu_0\right)\sqrt{n_2}}{\sigma_0}-\frac{\hat{\sigma}_0}{\sigma_0}\left(c_2L_{22}+\hat{W}_{1i}\sqrt{\frac{n_1}{n_2}}\right)+\delta\sqrt{n_2}\le\frac{\left(\bar{X}_{2i}-\mu_0+\delta\sigma_0\right)\sqrt{n_2}}{\sigma_0}\right.$$

$$\left.\le\frac{\left(\hat{\mu}_0-\mu_0\right)\sqrt{n_2}}{\sigma_0}-\frac{\hat{\sigma}_0}{\sigma_0}\left(c_2L_{21}+\hat{W}_{1i}\sqrt{\frac{n_1}{n_2}}\right)+\delta\sqrt{n_2}\right)$$

$$=\Phi\left[U\sqrt{\frac{n_2}{mn}}-V\left(c_2L_{21}+\hat{W}_{1i}\sqrt{\frac{n_1}{n_2}}\right)+\delta\sqrt{n_2}\right]-\Phi\left[U\sqrt{\frac{n_2}{mn}}-V\left(c_2L_{22}+\hat{W}_{1i}\sqrt{\frac{n_1}{n_2}}\right)+\delta\sqrt{n_2}\right],$$

as $U=\left(\hat{\mu}_0-\mu_0\right)\frac{\sqrt{mn}}{\sigma_0}$ and $V=\frac{\hat{\sigma}_0}{\sigma_0}$ (see Equations (15) and (16), respectively).

Similarly, it can be shown that

$$\Pr\left(L_{21} \le \hat{W}_{2i} \le L_{22}\right)$$

$$= \Phi\left[U\sqrt{\frac{n_2}{mn}} + V\left(c_2 L_{22} - \hat{W}_{1i}\sqrt{\frac{n_1}{n_2}}\right) + \delta\sqrt{n_2}\right] - \Phi\left[U\sqrt{\frac{n_2}{mn}} + V\left(c_2 L_{21} - \hat{W}_{1i}\sqrt{\frac{n_1}{n_2}}\right) + \delta\sqrt{n_2}\right].$$

Therefore, Equation (B11) becomes

$$\Pr\left(\hat{W}_{2i} \in I_{22}\right)$$

$$= \Phi\left[U\sqrt{\frac{n_2}{mn}} + V\left(c_2 L_{22} - \hat{W}_{1i}\sqrt{\frac{n_1}{n_2}}\right) + \delta\sqrt{n_2}\right] - \Phi\left[U\sqrt{\frac{n_2}{mn}} + V\left(c_2 L_{21} - \hat{W}_{1i}\sqrt{\frac{n_1}{n_2}}\right) + \delta\sqrt{n_2}\right] +$$

$$\Phi\left[U\sqrt{\frac{n_2}{mn}} - V\left(c_2 L_{21} + \hat{W}_{1i}\sqrt{\frac{n_1}{n_2}}\right) + \delta\sqrt{n_2}\right] - \Phi\left[U\sqrt{\frac{n_2}{mn}} - V\left(c_2 L_{22} + \hat{W}_{1i}\sqrt{\frac{n_1}{n_2}}\right) + \delta\sqrt{n_2}\right].$$

(B12)

By incorporating the results in Equations (B11) and (B12) into Equation (B10) gives

$$\hat{P}_3 = \int_{w_1 \in I_{12}} \left[\Phi\left(U\sqrt{\frac{n_2}{mn}} + V\left(c_2 L_{22} - w_1\sqrt{\frac{n_1}{n_2}}\right) + \delta\sqrt{n_2}\right)\right.$$

$$\left. - \Phi\left(U\sqrt{\frac{n_2}{mn}} + V\left(c_2 L_{21} - w_1\sqrt{\frac{n_1}{n_2}}\right) + \delta\sqrt{n_2}\right)\right] f_{\hat{W}_{1i}}\left(w_1 \middle| \hat{\mu}_0, \hat{\sigma}_0\right) \mathrm{d}w_1$$

$$+ \int_{w_1 \in I_{12}} \left[\Phi\left(U\sqrt{\frac{n_2}{mn}} - V\left(c_2 L_{21} + w_1\sqrt{\frac{n_1}{n_2}}\right) + \delta\sqrt{n_2}\right)\right.$$

$$\left. - \Phi\left(U\sqrt{\frac{n_2}{mn}} - V\left(c_2 L_{22} + w_1\sqrt{\frac{n_1}{n_2}}\right) + \delta\sqrt{n_2}\right)\right] f_{\hat{W}_{1i}}\left(w_1 \middle| \hat{\mu}_0, \hat{\sigma}_0\right) \mathrm{d}w_1 . \quad \text{(B13)}$$

Note that $c_2$ is defined in Appendix A. This completes the formulae derivation of $\hat{P}_3$ in Equation (24).

Table 1 A summary of the statistics used in the 11 steps procedure in Section 2 and their distributions

| Inspection Level 1 | Inspection Level 2 | Inspection Level 3 |
|---|---|---|
| $\bar{X}_{1i} = \frac{1}{n_1}\sum_{j=1}^{n_1} X_{1i,j}$ $\sim N\left(\mu_0 - \delta\sigma_0, \frac{\sigma_0^2}{n_1}\right)$ | $\bar{X}_{2i} = \frac{1}{n_2}\sum_{j=1}^{n_2} X_{2i,j}$ $\sim N\left(\mu_0 - \delta\sigma_0, \frac{\sigma_0^2}{n_2}\right)$ | $\bar{X}_{3i} = \frac{1}{n_3}\sum_{j=1}^{n_3} X_{3i,j}$ $\sim N\left(\mu_0 - \delta\sigma_0, \frac{\sigma_0^2}{n_3}\right)$ |
| $Y_{1i} = \bar{X}_{1i}$ $\sim N\left(\mu_0 - \delta\sigma_0, \frac{\sigma_0^2}{n_1}\right)$ | $Y_{2i} = \frac{n_1\bar{X}_{1i} + n_2\bar{X}_{2i}}{n_1 + n_2}$ $\sim N\left(\mu_0 - \delta\sigma_0, \frac{\sigma_0^2}{n_1 + n_2}\right)$ | $Y_{3i} = \frac{n_1\bar{X}_{1i} + n_2\bar{X}_{2i} + n_3\bar{X}_{3i}}{n_1 + n_2 + n_3}$ $\sim N\left(\mu_0 - \delta\sigma_0, \frac{\sigma_0^2}{n_1 + n_2 + n_3}\right)$ |
| $W_{1i} = \frac{(Y_{1i} - \mu_0)\sqrt{n_1}}{\sigma_0}$ $\sim N\left(-\delta\sqrt{n_1}, 1\right)$ | $W_{2i} = \frac{(Y_{2i} - \mu_0)\sqrt{n_1 + n_2}}{\sigma_0}$ $\sim N\left(-\delta\sqrt{n_1 + n_2}, 1\right)$ | $W_{3i} = \frac{(Y_{3i} - \mu_0)\sqrt{n_1 + n_2 + n_3}}{\sigma_0}$ $\sim N\left(-\delta\sqrt{n_1 + n_2 + n_3}, 1\right)$ |

Table 2. ARL(0) values of the (i) $TS_K\ \bar{X}$ chart adopted from He, Grigoryan, and Sigh (2002), (ii) revised $TS_K\ \bar{X}$ chart computed using MATLAB based on the model in Section 3.1, (iii) revised $TS_K\ \bar{X}$ chart simulated using SAS; and the 95% confidence interval for ARL(0) of the revised $TS_K\ \bar{X}$ chart simulated using SAS; all obtained using the parameters in He, Grigoryan, and Sigh (2002)

| ARL(0) (adopted from He, Grigoryan, and Sigh, 2002) | $n_1$ | $n_2$ | $n_3$ | $L_{11}$ | $L_{12}$ | $L_{21}$ | $L_{22}$ | $L_3$ | ARL(0) (proposed model) | ARL(0) (simulated) | 95% confidence interval for ARL(0) |
|---|---|---|---|---|---|---|---|---|---|---|---|
| 370.40 | 1 | 1 | 1 | 1.62 | 3.07 | 1.80 | 3.35 | 2.86 | 221.11 | 222.72 | (218.08, 223.79) |
| 500.00 | 1 | 1 | 1 | 1.79 | 3.00 | 1.80 | 3.01 | 2.93 | 192.90 | 193.97 | (190.28, 195.06) |
| 370.40 | 2 | 1 | 1 | 1.76 | 3.00 | 1.80 | 3.69 | 2.66 | 142.87 | 143.92 | (140.80, 144.64) |
| 500.00 | 2 | 2 | 1 | 1.80 | 3.00 | 1.80 | 3.39 | 2.85 | 203.36 | 204.24 | (200.13, 205.94) |
| 370.40 | 2 | 2 | 1 | 1.47 | 3.00 | 1.80 | 3.30 | 2.87 | 181.96 | 182.41 | (179.15, 184.51) |
| 500.00 | 2 | 2 | 2 | 1.49 | 3.00 | 1.47 | 4.51 | 2.81 | 182.62 | 181.31 | (180.09, 184.86) |
| 370.40 | 2 | 2 | 3 | 1.23 | 3.32 | 1.55 | 3.90 | 2.81 | 248.04 | 251.01 | (244.30, 251.10) |
| 500.00 | 2 | 2 | 3 | 1.34 | 3.67 | 1.56 | 3.14 | 2.88 | 268.96 | 269.97 | (265.13, 272.38) |
| 370.40 | 3 | 3 | 2 | 1.57 | 3.00 | 1.80 | 3.61 | 2.81 | 181.94 | 183.27 | (179.19, 184.51) |
| 500.00 | 3 | 3 | 2 | 1.66 | 3.00 | 1.80 | 3.86 | 2.87 | 204.89 | 207.40 | (201.55, 207.42) |
| 370.40 | 3 | 3 | 4 | 1.41 | 3.00 | 1.61 | 4.07 | 2.86 | 198.33 | 199.22 | (195.38, 200.88) |
| 500.00 | 3 | 3 | 5 | 1.48 | 3.17 | 1.80 | 3.44 | 2.89 | 274.00 | 270.93 | (270.64, 277.15) |
| 370.40 | 4 | 4 | 3 | 1.63 | 3.00 | 1.66 | 3.14 | 2.84 | 178.51 | 177.64 | (175.92, 181.13) |
| 500.00 | 3 | 3 | 4 | 1.32 | 3.72 | 1.68 | 3.56 | 2.82 | 299.61 | 300.01 | (295.43, 304.17) |
| 370.40 | 4 | 4 | 6 | 1.49 | 3.13 | 1.78 | 3.09 | 2.91 | 216.02 | 217.64 | (212.60, 218.96) |
| 500.00 | 4 | 5 | 4 | 1.59 | 3.00 | 1.80 | 3.39 | 2.97 | 226.34 | 228.44 | (221.89, 229.40) |
| 370.40 | 5 | 8 | 3 | 1.55 | 3.00 | 1.80 | 3.57 | 2.89 | 209.76 | 208.24 | (206.72, 212.69) |
| 500.00 | 5 | 5 | 6 | 1.43 | 3.36 | 1.80 | 3.81 | 2.98 | 387.66 | 391.44 | (380.73, 393.23) |
| 370.40 | 8 | 10 | 5 | 1.49 | 3.00 | 1.67 | 3.18 | 2.72 | 150.77 | 150.67 | (149.23, 152.68) |
| 500.00 | 8 | 5 | 7 | 1.54 | 3.09 | 1.71 | 3.74 | 2.76 | 184.47 | 186.86 | (182.06, 187.03) |

Table 3. Optimal parameters $(n_1, n_2, n_3, L_{11}, L_{12}\ L_{21}, L_{22}, L_3)$ and the corresponding ANOS($\delta$) values for the revised $\mathrm{TS}_K\ \bar{X}$ chart, and ANOS($\delta$) values for the optimal $\mathrm{DS}_K\ \bar{X}$ chart with the percentage of a decrease in the ANOS($\delta$) value by using the revised $\mathrm{TS}_K\ \bar{X}$ chart in place of the $\mathrm{DS}_K\ \bar{X}$ chart

| $n_0$ | $\delta$ | $\mathrm{TS}_K\ \bar{X}$ | | | | | | | | | $\mathrm{DS}_K\ \bar{X}$ | Decrease (%) |
|---|---|---|---|---|---|---|---|---|---|---|---|---|
| | | $n_1$ | $n_2$ | $n_3$ | $L_{11}$ | $L_{12}$ | $L_{21}$ | $L_{22}$ | $L_3$ | ANOS($\delta$) | ANOS($\delta$) | |
| 5 | 0.1 | 3 | 5 | 10 | 1.20 | 4.27 | 1.3099 | 4.00 | 2.0614 | 253.41 | *270.17* | 6.20 |
| | 0.2 | 3 | 5 | 10 | 1.20 | 4.69 | 1.3071 | 3.53 | 2.0654 | 130.17 | *147.41* | 11.70 |
| | 0.3 | 3 | 5 | 10 | 1.20 | 4.30 | 1.3063 | 3.49 | 2.0667 | 72.79 | *82.41* | 11.67 |
| | 0.5 | 3 | 5 | 9 | 1.15 | 4.04 | 1.3256 | 2.77 | 2.2096 | 32.09 | *34.65* | 7.39 |
| | 0.7 | 3 | 5 | 5 | 0.97 | 3.35 | 1.5464 | 2.69 | 2.3864 | 18.50 | *25.48* | 27.39 |
| | 1 | 4 | 3 | 3 | 1.06 | 2.88 | 1.8102 | 2.71 | 2.5699 | 10.13 | *10.48* | 3.34 |
| | 1.5 | 4 | 2 | 2 | 0.71 | 2.65 | 2.0490 | 2.76 | 2.7871 | 5.34 | *5.33* | -0.19 |
| | 2 | 3 | 3 | 8 | 1.29 | 2.61 | 0.1008 | 2.81 | 2.8916 | 3.69 | *3.60* | -2.50 |
| 7 | 0.1 | 4 | 7 | 14 | 1.21 | 4.36 | 1.1343 | 3.49 | 1.8969 | 239.09 | *254.75* | 6.15 |
| | 0.2 | 5 | 7 | 14 | 1.39 | 4.20 | 1.3982 | 2.75 | 1.8393 | 121.28 | *131.47* | 7.75 |
| | 0.3 | 4 | 7 | 14 | 1.20 | 4.20 | 1.1299 | 2.80 | 1.9574 | 66.97 | *73.25* | 8.57 |
| | 0.5 | 5 | 5 | 7 | 1.10 | 3.32 | 1.3887 | 2.70 | 2.2024 | 31.28 | *32.76* | 4.52 |
| | 0.7 | 6 | 4 | 3 | 1.23 | 2.83 | 1.7553 | 2.62 | 2.3436 | 17.98 | *18.96* | 5.17 |
| | 1 | 6 | 3 | 3 | 1.34 | 2.61 | 0.2064 | 2.61 | 2.5337 | 9.99 | *10.39* | 3.85 |
| | 1.5 | 5 | 3 | 8 | 1.21 | 2.47 | 0.6710 | 2.60 | 3.4207 | 5.88 | *5.44* | -8.09 |
| | 2 | 4 | 3 | 14 | 1.26 | 2.41 | 0.3336 | 2.76 | 3.6524 | 4.22 | *3.70* | -14.05 |

Table 4. Optimal parameters $(n_1, n_2, n_3, L_{11}, L_{12}\ L_{21}, L_{22}, L_3)$ and the corresponding ARL($\delta$) values for the revised $\mathrm{TS}_K\ \bar{X}$ chart based on ARL(0) = 370, and ARL($\delta$) values for the optimal $\mathrm{DS}_K\ \bar{X}$, $\mathrm{AS}_3\ \bar{X}$ and $\mathrm{AS}_2\ \bar{X}$ charts with the percentage of a decrease in the ARL($\delta$) value by using the revised $\mathrm{TS}_K\ \bar{X}$ chart in place of the competing charts

| $n_0$ | $\delta$ | $\mathrm{TS}_K\ \bar{X}$ | | | | | | | | | $\mathrm{DS}_K\ \bar{X}$ | | $\mathrm{AS}_3\ \bar{X}$ | | $\mathrm{AS}_2\ \bar{X}$ | |
|---|---|---|---|---|---|---|---|---|---|---|---|---|---|---|---|---|
| | | $n_1$ | $n_2$ | $n_3$ | $L_{11}$ | $L_{12}$ | $L_{21}$ | $L_{22}$ | $L_3$ | ARL($\delta$) | ARL($\delta$) | Decrease (%) | ARL($\delta$) | Decrease (%) | ARL($\delta$) | Decrease (%) |
| 5 | 0.1 | 4 | 5 | 10 | 1.54 | 4.84 | 1.7015 | 4.60 | 2.6813 | 199.65 | *218.00* | 8.42 | 293.07 | 31.88 | 293.39 | 31.95 |
| | 0.2 | 4 | 5 | 10 | 1.54 | 4.94 | 1.7015 | 4.63 | 2.6812 | 72.46 | *86.40* | 16.13 | 162.65 | 55.45 | 163.97 | 55.81 |
| | 0.3 | 4 | 5 | 10 | 1.53 | 5.17 | 1.7317 | 4.42 | 2.6802 | 29.09 | *36.30* | 19.86 | 77.58 | 62.50 | 78.63 | 63.00 |
| | 0.5 | 3 | 5 | 10 | 1.11 | 4.94 | 1.5506 | 3.94 | 2.7784 | 7.04 | *9.20* | 23.48 | 18.21 | 61.34 | 18.30 | 61.53 |
| | 0.7 | 3 | 5 | 10 | 1.09 | 5.05 | 1.6058 | 4.75 | 2.7695 | 2.84 | *3.60* | 21.11 | 6.17 | 53.97 | 6.17 | 53.97 |
| | 1 | 3 | 4 | 10 | 0.94 | 5.13 | 1.7209 | 4.79 | 2.7773 | 1.46 | *1.70* | 14.12 | 2.57 | 43.19 | 2.58 | 43.41 |
| | 1.5 | 3 | 3 | 7 | 0.74 | 4.94 | 1.6076 | 4.58 | 2.8820 | 1.05 | *1.10* | 4.55 | 1.43 | 26.57 | 1.46 | 28.08 |
| | 2 | 4 | 1 | 5 | 0.92 | 4.73 | 1.4838 | 4.42 | 2.9483 | 1.00 | *1.00* | 0 | 1.08 | 7.41 | 1.10 | 9.09 |
| 7 | 0.1 | 5 | 7 | 14 | 1.34 | 4.93 | 1.5999 | 4.86 | 2.7369 | 165.38 | *191.48* | 13.63 | 268.26 | 38.35 | 268.86 | 38.49 |
| | 0.2 | 5 | 7 | 14 | 1.33 | 4.91 | 1.6284 | 4.65 | 2.7360 | 50.38 | *66.48* | 24.22 | 124.29 | 59.47 | 125.89 | 59.98 |
| | 0.3 | 5 | 7 | 14 | 1.33 | 4.91 | 1.6284 | 4.85 | 2.7359 | 18.35 | *25.86* | 29.04 | 50.58 | 63.72 | 51.35 | 64.26 |
| | 0.5 | 5 | 7 | 14 | 1.31 | 5.13 | 1.6857 | 4.72 | 2.7328 | 4.39 | *6.11* | 28.15 | 10.43 | 57.91 | 10.44 | 57.95 |
| | 0.7 | 4 | 7 | 14 | 1.05 | 4.93 | 1.5658 | 4.65 | 2.7768 | 1.98 | *2.48* | 20.16 | 3.89 | 49.10 | 3.89 | 49.10 |
| | 1 | 5 | 5 | 12 | 1.11 | 5.14 | 1.7626 | 4.77 | 2.8000 | 1.21 | *1.32* | 8.33 | 1.95 | 37.95 | 1.96 | 38.27 |
| | 1.5 | 5 | 4 | 10 | 0.91 | 3.38 | 1.8386 | 3.40 | 3.0284 | 1.01 | *1.02* | 0.98 | 1.18 | 14.41 | 1.20 | 15.83 |
| | 2 | 6 | 4 | 10 | 1.24 | 3.25 | 2.3497 | 3.11 | 3.9101 | 1.00 | *1.00* | 0 | 1.01 | 0.99 | 1.02 | 1.96 |

Table 5. Optimal parameters $(n_1, n_2, n_3, L_{11}, L_{12}\ L_{21}, L_{22}, L_3)$ of the revised $\mathrm{TS}_E$ $\bar{X}$ chart when AANOS(0) = 370, $n_0 \in \{5, 7\}$ and $m \in \{20, 40, 80\}$

| $m$ | $\delta$ | $n_0$= 5 | | | | | | | | $n_0$ = 7 | | | | | | | |
|---|---|---|---|---|---|---|---|---|---|---|---|---|---|---|---|---|---|
| | | $n_1$ | $n_2$ | $n_3$ | $L_{11}$ | $L_{12}$ | $L_{21}$ | $L_{22}$ | $L_3$ | $n_1$ | $n_2$ | $n_3$ | $L_{11}$ | $L_{12}$ | $L_{21}$ | $L_{22}$ | $L_3$ |
| 20 | 0.1 | 3 | 5 | 10 | 1.24 | 4.25 | 1.3554 | 3.51 | 2.1646 | 4 | 7 | 14 | 1.21 | 4.25 | 1.2647 | 3.31 | 2.0137 |
| | 0.2 | 3 | 5 | 10 | 1.23 | 4.25 | 1.3796 | 3.41 | 2.1668 | 4 | 7 | 14 | 1.20 | 4.28 | 1.2838 | 3.15 | 2.0227 |
| | 0.3 | 3 | 5 | 10 | 1.23 | 4.25 | 1.3747 | 3.30 | 2.1728 | 4 | 7 | 14 | 1.20 | 4.34 | 1.2630 | 2.91 | 2.0552 |
| | 0.5 | 3 | 5 | 10 | 1.21 | 3.91 | 1.3851 | 2.84 | 2.2561 | 3 | 7 | 11 | 1.20 | 3.75 | 0.1295 | 2.59 | 2.1806 |
| | 0.7 | 4 | 4 | 5 | 1.38 | 3.10 | 1.5982 | 2.75 | 2.3978 | 5 | 5 | 4 | 0.95 | 2.90 | 1.7046 | 2.67 | 2.4089 |
| | 1 | 4 | 3 | 3 | 1.09 | 2.88 | 1.8424 | 2.72 | 2.5852 | 6 | 2 | 2 | 0.85 | 2.70 | 1.5919 | 2.70 | 2.4939 |
| | 1.5 | 4 | 2 | 2 | 1.10 | 2.69 | 0.6334 | 2.70 | 2.7922 | 5 | 3 | 4 | 0.94 | 2.60 | 0.7495 | 2.54 | 2.9145 |
| | 2 | 3 | 2 | 6 | 1.12 | 2.60 | 0.1356 | 2.70 | 3.4041 | 3 | 3 | 11 | 1.01 | 2.50 | 0.1370 | 2.59 | 3.7736 |
| 40 | 0.1 | 3 | 5 | 10 | 1.22 | 4.55 | 1.3341 | 3.63 | 2.1289 | 4 | 7 | 14 | 1.20 | 4.22 | 1.2292 | 3.42 | 1.9680 |
| | 0.2 | 3 | 5 | 10 | 1.22 | 4.62 | 1.3338 | 3.61 | 2.1292 | 4 | 7 | 14 | 1.19 | 4.62 | 1.2496 | 3.20 | 1.9761 |
| | 0.3 | 3 | 5 | 10 | 1.22 | 4.24 | 1.3256 | 3.30 | 2.1412 | 4 | 7 | 14 | 1.18 | 4.31 | 1.2508 | 2.85 | 2.0221 |
| | 0.5 | 3 | 5 | 10 | 1.20 | 3.95 | 1.3399 | 2.80 | 2.2384 | 3 | 7 | 9 | 0.82 | 3.90 | 1.2441 | 2.67 | 2.2364 |
| | 0.7 | 4 | 4 | 4 | 1.30 | 3.15 | 1.6871 | 2.76 | 2.3939 | 6 | 3 | 4 | 1.18 | 2.91 | 1.6620 | 2.66 | 2.3780 |
| | 1 | 4 | 3 | 3 | 1.10 | 2.90 | 1.7262 | 2.73 | 2.5807 | 6 | 2 | 2 | 0.75 | 2.68 | 1.8874 | 2.65 | 2.4739 |
| | 1.5 | 4 | 2 | 4 | 1.35 | 2.70 | 0.3648 | 2.70 | 2.8059 | 5 | 3 | 4 | 1.03 | 2.48 | 0.1157 | 2.65 | 3.0472 |
| | 2 | 3 | 3 | 8 | 1.25 | 2.60 | 0.4394 | 2.80 | 3.0222 | 3 | 3 | 11 | 1.01 | 2.47 | 0.1154 | 2.64 | 3.7909 |
| 80 | 0.1 | 3 | 5 | 10 | 1.20 | 4.74 | 1.3473 | 3.55 | 2.1028 | 4 | 7 | 14 | 1.20 | 4.66 | 1.1954 | 3.41 | 1.9386 |
| | 0.2 | 3 | 5 | 10 | 1.21 | 4.45 | 1.3209 | 3.61 | 2.1033 | 4 | 7 | 14 | 1.20 | 4.64 | 1.1865 | 3.14 | 1.9513 |
| | 0.3 | 3 | 5 | 10 | 1.20 | 4.45 | 1.3393 | 3.24 | 2.1171 | 4 | 7 | 14 | 1.20 | 4.31 | 1.1783 | 3.00 | 1.9654 |
| | 0.5 | 4 | 5 | 10 | 1.54 | 3.34 | 1.6167 | 2.58 | 2.1562 | 3 | 7 | 9 | 1.04 | 3.94 | 0.4830 | 2.60 | 2.1911 |
| | 0.7 | 4 | 4 | 4 | 1.30 | 3.15 | 1.6273 | 2.73 | 2.3977 | 6 | 3 | 4 | 1.20 | 2.91 | 1.5759 | 2.65 | 2.3726 |
| | 1 | 3 | 4 | 6 | 1.25 | 2.90 | 0.1142 | 2.59 | 2.6476 | 6 | 2 | 2 | 0.75 | 2.67 | 1.8577 | 2.65 | 2.4736 |
| | 1.5 | 4 | 4 | 10 | 1.29 | 2.69 | 1.9924 | 2.60 | 3.6364 | 5 | 3 | 4 | 1.03 | 2.68 | 0.1457 | 2.48 | 2.8299 |
| | 2 | 3 | 3 | 8 | 1.20 | 2.70 | 0.6610 | 2.70 | 2.8553 | 3 | 3 | 11 | 1.01 | 2.47 | 0.1056 | 2.64 | 3.6599 |

Table 6. AANOS($\delta$) and SDANOS($\delta$) values for the optimal revised $TS_E\ \bar{X}$ and $DS_E\ \bar{X}$ charts with the percentage of reduction in AANOS($\delta$) when AANOS(0) = 370, $n_0 \in \{5, 7\}$ and $m \in \{20, 40, 80\}$

| $n_0$ | $\delta$ | $m = 20$ | | | | | $m = 40$ | | | | | $m = 80$ | | | | |
|---|---|---|---|---|---|---|---|---|---|---|---|---|---|---|---|---|
| | | $TS_E\ \bar{X}$ | | $DS_E\ \bar{X}$ | | | $TS_E\ \bar{X}$ | | $DS_E\ \bar{X}$ | | | $TS_E\ \bar{X}$ | | $DS_E\ \bar{X}$ | | |
| | | AANOS($\delta$) | SDANOS($\delta$) | AANOS($\delta$) | SDANOS($\delta$) | Decrease (%) | AANOS($\delta$) | SDANOS($\delta$) | AANOS($\delta$) | SDANOS($\delta$) | Decrease (%) | AANOS($\delta$) | SDANOS($\delta$) | AANOS($\delta$) | SDANOS($\delta$) | Decrease (%) |
| 5 | 0.1 | 308.79 | 189.42 | 314.22 | 202.44 | 1.73 | 291.05 | 127.62 | 300.32 | 133.88 | 3.09 | 276.49 | 89.79 | 289.06 | 92.28 | 4.35 |
| | 0.2 | 191.78 | 145.93 | 204.11 | 154.76 | 6.04 | 164.16 | 88.12 | 180.09 | 94.79 | 8.85 | 147.81 | 54.83 | 165.52 | 60.27 | 10.70 |
| | 0.3 | 105.17 | 83.05 | 116.54 | 91.80 | 9.76 | 88.33 | 49.91 | 100.16 | 49.64 | 11.81 | 80.36 | 24.97 | 91.94 | 29.99 | 12.60 |
| | 0.5 | 38.84 | 19.56 | 42.46 | 22.91 | 8.53 | 35.40 | 10.43 | 38.60 | 12.36 | 8.29 | 35.03 | 7.13 | 36.74 | 7.67 | 4.65 |
| | 0.7 | 20.74 | 7.49 | 22.29 | 6.99 | 6.95 | 19.80 | 4.61 | 21.21 | 4.46 | 6.65 | 19.26 | 3.02 | 20.64 | 2.89 | 6.69 |
| | 1 | 10.63 | 2.60 | 11.36 | 3.04 | 6.43 | 10.41 | 1.68 | 11.10 | 1.97 | 6.22 | 10.51 | 1.10 | 10.95 | 1.33 | 4.02 |
| | 1.5 | 5.45 | 0.68 | 5.42 | 0.90 | –0.55 | 5.48 | 0.45 | 5.38 | 0.62 | –1.86 | 5.89 | 0.36 | 5.36 | 0.43 | –9.89 |
| | 2 | 3.61 | 0.30 | 3.60 | 0.46 | –0.28 | 3.70 | 0.22 | 3.60 | 0.33 | –2.78 | 3.76 | 0.16 | 3.60 | 0.23 | –4.44 |
| 7 | 0.1 | 294.34 | 151.16 | 300.77 | 156.03 | 2.14 | 275.08 | 106.46 | 285.01 | 107.70 | 3.48 | 260.29 | 75.95 | 273.14 | 75.96 | 4.70 |
| | 0.2 | 167.04 | 109.57 | 178.52 | 114.17 | 6.43 | 143.83 | 65.76 | 157.24 | 70.38 | 8.53 | 131.27 | 40.73 | 145.36 | 44.72 | 9.69 |
| | 0.3 | 88.60 | 54.47 | 96.85 | 59.70 | 8.52 | 77.30 | 28.85 | 85.29 | 32.84 | 9.37 | 72.25 | 17.04 | 79.68 | 20.41 | 9.32 |
| | 0.5 | 35.25 | 12.99 | 37.84 | 13.67 | 6.84 | 33.10 | 7.70 | 35.41 | 7.89 | 6.52 | 31.93 | 5.03 | 34.22 | 5.03 | 6.69 |
| | 0.7 | 19.50 | 5.35 | 20.56 | 5.70 | 5.16 | 18.81 | 3.50 | 19.79 | 3.64 | 4.95 | 18.42 | 2.34 | 19.39 | 2.42 | 5.00 |
| | 1 | 10.49 | 1.90 | 10.82 | 1.94 | 3.05 | 10.25 | 1.23 | 10.62 | 1.27 | 3.48 | 10.15 | 0.84 | 10.51 | 0.87 | 3.43 |
| | 1.5 | 5.93 | 0.40 | 5.53 | 0.57 | –7.23 | 5.84 | 0.27 | 5.49 | 0.39 | –6.38 | 5.94 | 0.19 | 5.47 | 0.27 | –8.59 |
| | 2 | 3.61 | 0.24 | 3.73 | 0.27 | 3.22 | 3.59 | 0.16 | 3.73 | 0.18 | 3.75 | 3.58 | 0.11 | 3.72 | 0.13 | 3.76 |

Table 7. Optimal parameters ($n_1$, $n_2$, $n_3$, $L_{11}$, $L_{12}$ $L_{21}$, $L_{22}$, $L_3$) of the revised TS$_E$ $\bar{X}$ chart when AARL(0) = 370, $n_0 \in \{5, 7\}$ and $m \in \{20, 40, 80\}$

| $m$ | $\delta$ | $n_0$= 5 | | | | | | | | $n_0$ = 7 | | | | | | | |
|---|---|---|---|---|---|---|---|---|---|---|---|---|---|---|---|---|---|
| | | $n_1$ | $n_2$ | $n_3$ | $L_{11}$ | $L_{12}$ | $L_{21}$ | $L_{22}$ | $L_3$ | $n_1$ | $n_2$ | $n_3$ | $L_{11}$ | $L_{12}$ | $L_{21}$ | $L_{22}$ | $L_3$ |
| 20 | 0.1 | 4 | 5 | 10 | 1.61 | 4.87 | 1.7627 | 4.28 | 2.7185 | 5 | 7 | 14 | 1.39 | 4.91 | 1.6540 | 4.62 | 2.8126 |
| | 0.2 | 4 | 5 | 10 | 1.61 | 4.91 | 1.7630 | 4.33 | 2.7182 | 5 | 7 | 14 | 1.38 | 4.93 | 1.6826 | 4.63 | 2.8118 |
| | 0.3 | 4 | 5 | 10 | 1.60 | 5.40 | 1.7939 | 4.43 | 2.7167 | 5 | 7 | 14 | 1.38 | 4.88 | 1.6827 | 4.85 | 2.8117 |
| | 0.5 | 3 | 5 | 10 | 1.16 | 4.83 | 1.5825 | 4.87 | 2.8190 | 5 | 7 | 14 | 1.36 | 5.06 | 1.7399 | 4.73 | 2.8090 |
| | 0.7 | 3 | 5 | 10 | 1.14 | 5.03 | 1.6365 | 4.48 | 2.8167 | 4 | 7 | 14 | 1.07 | 5.05 | 1.6558 | 4.85 | 2.8505 |
| | 1 | 3 | 4 | 10 | 1.03 | 4.73 | 1.6626 | 4.46 | 2.8321 | 5 | 5 | 13 | 1.17 | 4.85 | 1.8259 | 4.15 | 2.8483 |
| | 1.5 | 3 | 3 | 7 | 0.78 | 4.73 | 1.6324 | 4.20 | 2.9056 | 5 | 4 | 10 | 0.96 | 3.45 | 1.8532 | 3.45 | 3.0188 |
| | 2 | 4 | 1 | 5 | 0.97 | 4.32 | 1.5210 | 4.11 | 2.9497 | 6 | 4 | 10 | 1.29 | 3.1 | 2.3699 | 3.25 | 3.8186 |
| 40 | 0.1 | 4 | 5 | 10 | 1.57 | 4.72 | 1.7474 | 4.37 | 2.7221 | 5 | 7 | 14 | 1.36 | 4.97 | 1.6416 | 4.85 | 2.7963 |
| | 0.2 | 4 | 5 | 10 | 1.57 | 5.08 | 1.7476 | 4.43 | 2.7217 | 5 | 7 | 14 | 1.36 | 4.97 | 1.6416 | 4.85 | 2.7963 |
| | 0.3 | 4 | 5 | 10 | 1.57 | 5.07 | 1.7478 | 4.57 | 2.7214 | 5 | 7 | 14 | 1.35 | 5.45 | 1.6701 | 4.85 | 2.7952 |
| | 0.5 | 3 | 5 | 10 | 1.13 | 4.54 | 1.5804 | 5.15 | 2.8170 | 5 | 7 | 14 | 1.34 | 5.12 | 1.6987 | 4.75 | 2.7939 |
| | 0.7 | 3 | 5 | 10 | 1.12 | 5.04 | 1.6078 | 4.83 | 2.8151 | 5 | 7 | 14 | 1.24 | 4.63 | 2.0064 | 4.31 | 2.7520 |
| | 1 | 3 | 4 | 11 | 1.02 | 5.19 | 1.6774 | 4.60 | 2.8064 | 5 | 5 | 12 | 1.13 | 4.95 | 1.7915 | 4.33 | 2.8513 |
| | 1.5 | 3 | 3 | 7 | 0.95 | 5.19 | 1.2740 | 4.61 | 2.9190 | 5 | 4 | 10 | 0.9 | 3.5 | 1.9241 | 3.5 | 2.9759 |
| | 2 | 4 | 1 | 5 | 0.94 | 5.15 | 1.5061 | 4.85 | 2.9583 | 6 | 7 | 10 | 1.1 | 3.3 | 3.5000 | 3.1 | 10.0000 |
| 80 | 0.1 | 4 | 5 | 10 | 1.55 | 5.16 | 1.7399 | 4.75 | 2.7116 | 5 | 7 | 14 | 1.35 | 5.2 | 1.6208 | 4.7 | 2.7764 |
| | 0.2 | 4 | 4 | 10 | 1.55 | 5.22 | 1.7399 | 4.73 | 2.7116 | 5 | 7 | 14 | 1.34 | 5.22 | 1.6493 | 4.74 | 2.7754 |
| | 0.3 | 4 | 5 | 10 | 1.55 | 5.22 | 1.7399 | 4.73 | 2.7116 | 5 | 7 | 14 | 1.34 | 5.22 | 1.6493 | 4.74 | 2.7754 |
| | 0.5 | 3 | 5 | 10 | 1.12 | 5.04 | 1.5659 | 4.72 | 2.8040 | 5 | 7 | 14 | 1.34 | 5.12 | 1.6987 | 4.75 | 2.7939 |
| | 0.7 | 3 | 5 | 11 | 1.08 | 5.13 | 1.7340 | 4.85 | 2.7681 | 4 | 7 | 14 | 1.04 | 5.33 | 1.6295 | 4.87 | 2.8117 |
| | 1 | 3 | 4 | 11 | 1.01 | 5.08 | 1.6638 | 4.75 | 2.7938 | 5 | 5 | 12 | 1.12 | 5.05 | 1.7772 | 4.58 | 2.8335 |
| | 1.5 | 3 | 2 | 7 | 0.75 | 4.96 | 1.3206 | 4.85 | 2.9296 | 5 | 3 | 10 | 0.9 | 3.5 | 1.6377 | 3.5 | 3.0069 |
| | 2 | 4 | 2 | 5 | 1.00 | 4.20 | 1.7613 | 3.85 | 2.9383 | 6 | 3 | 9 | 1.18 | 3.15 | 2.1034 | 3.22 | 3.5846 |

Table 8. AARL($\delta$) and SDARL($\delta$) values for the optimal revised $TS_E\ \bar{X}$ and $DS_E\ \bar{X}$ charts, and the percentage of a decrease in the AARL($\delta$) value by using the $TS_E\ \bar{X}$ chart in place of the $DS_E\ \bar{X}$ chart when AARL(0) = 370, $n_0 \in \{5, 7\}$ and $m \in \{20, 40, 80\}$

| $n_0$ | $\delta$ | $m$ = 20 | | | | | $m$ = 40 | | | | | $m$ = 80 | | | | |
|---|---|---|---|---|---|---|---|---|---|---|---|---|---|---|---|---|
| | | $TS_E\ \bar{X}$ | | $DS_E\ \bar{X}$ | | | $TS_E\ \bar{X}$ | | $DS_E\ \bar{X}$ | | | $TS_E\ \bar{X}$ | | $DS_E\ \bar{X}$ | | |
| | | AARL($\delta$) | SDARL($\delta$) | AARL($\delta$) | SDARL($\delta$) | Decrease (%) | AARL($\delta$) | SDARL($\delta$) | AARL($\delta$) | SDARL($\delta$) | Decrease (%) | AARL($\delta$) | SDARL($\delta$) | AARL($\delta$) | SDARL($\delta$) | Decrease (%) |
| 5 | 0.1 | 290.18 | 327.47 | 296.24 | 348.75 | 2.05 | 263.13 | 198.18 | 275.40 | 207.22 | 4.46 | 239.03 | 130.18 | 256.99 | 134.17 | 6.99 |
| | 0.2 | 149.22 | 212.88 | 163.14 | 227.39 | 8.53 | 113.63 | 107.34 | 131.91 | 118.10 | 13.86 | 92.54 | 58.42 | 113.37 | 67.02 | 18.37 |
| | 0.3 | 60.44 | 98.69 | 72.37 | 111.53 | 16.48 | 43.78 | 39.17 | 55.24 | 48.19 | 20.75 | 35.55 | 19.59 | 47.46 | 25.54 | 25.09 |
| | 0.5 | 10.76 | 12.46 | 14.74 | 16.84 | 27.00 | 8.72 | 5.09 | 12.31 | 7.44 | 29.16 | 7.86 | 2.84 | 11.22 | 4.27 | 29.95 |
| | 0.7 | 3.51 | 2.02 | 4.72 | 3.08 | 25.64 | 3.17 | 1.04 | 4.30 | 1.64 | 26.28 | 2.94 | 0.60 | 4.09 | 1.01 | 28.12 |
| | 1 | 1.56 | 0.31 | 1.83 | 0.48 | 14.75 | 1.50 | 0.18 | 1.77 | 0.29 | 15.25 | 1.48 | 0.10 | 1.74 | 0.19 | 14.94 |
| | 1.5 | 1.06 | 0.04 | 1.09 | 0.06 | 2.75 | 1.06 | 0.02 | 1.09 | 0.04 | 2.75 | 1.05 | 0.02 | 1.08 | 0.02 | 2.78 |
| | 2 | 1.00 | 0.00 | 1.00 | 0.01 | 0.00 | 1.00 | 0.00 | 1.00 | 0.00 | 0.00 | 1.00 | 0.00 | 1.00 | 0.00 | 0.00 |
| 7 | 0.1 | 263.92 | 264.69 | 273.57 | 271.31 | 3.53 | 230.97 | 167.95 | 247.20 | 168.10 | 6.57 | 204.39 | 256.84 | 225.99 | 110.98 | 9.56 |
| | 0.2 | 108.36 | 148.45 | 124.27 | 156.27 | 12.80 | 78.36 | 72.30 | 96.76 | 79.83 | 19.02 | 63.75 | 82.56 | 82.36 | 44.49 | 22.60 |
| | 0.3 | 35.79 | 53.11 | 46.18 | 61.15 | 22.50 | 25.83 | 38.39 | 35.50 | 26.38 | 27.24 | 21.89 | 26.00 | 30.90 | 14.30 | 29.16 |
| | 0.5 | 6.06 | 8.73 | 8.47 | 7.03 | 28.45 | 5.17 | 3.18 | 7.33 | 3.45 | 29.47 | 5.17 | 3.18 | 6.80 | 2.06 | 23.97 |
| | 0.7 | 2.26 | 2.02 | 2.88 | 1.24 | 21.53 | 2.17 | 1.72 | 2.70 | 0.71 | 19.63 | 2.05 | 1.52 | 2.61 | 0.45 | 21.46 |
| | 1 | 1.26 | 0.60 | 1.37 | 0.19 | 8.03 | 1.23 | 0.55 | 1.35 | 0.12 | 8.89 | 1.22 | 0.52 | 1.34 | 0.08 | 8.96 |
| | 1.5 | 1.01 | 0.12 | 1.02 | 0.02 | 0.98 | 1.01 | 1.01 | 1.02 | 0.01 | 0.98 | 1.01 | 1.01 | 1.02 | 0.01 | 0.98 |
| | 2 | 1.00 | 0.02 | 1.00 | 0.00 | 0.00 | 1.00 | 0.01 | 1.00 | 0.00 | 0.00 | 1.00 | 0.00 | 1.00 | 0.00 | 0.00 |

Table 9. AANOS(0) and SDANOS(0) values for the revised $TS_E$ $\bar{X}$ chart for different number of in-control Phase-I samples ($m$), computed using the optimal parameters of the revised $TS_K$ $\bar{X}$ chart in minimizing ANOS(1.5), based on $n_0 \in \{5, 7\}$ and ANOS(0) $\in \{200, 370\}$

| $m$ | ANOS(0) = 200 | | | | ANOS(0) = 370 | | | |
|---|---|---|---|---|---|---|---|---|
| | $n_0 = 5$ | | $n_0 = 7$ | | $n_0 = 5$ | | $n_0 = 7$ | |
| | AANOS(0) | SDANOS(0) | AANOS(0) | SDANOS(0) | AANOS(0) | SDANOS(0) | AANOS(0) | SDANOS(0) |
| 50 | 198.38 | 67.60 | 194.26 | 58.66 | 370.56 | 152.66 | 368.47 | 120.67 |
| 100 | 198.86 | 46.32 | 196.68 | 40.65 | 369.42 | 103.07 | 368.76 | 82.89 |
| 150 | 199.15 | 37.44 | 197.67 | 32.95 | 369.39 | 82.93 | 369.05 | 67.04 |
| 200 | 199.33 | 32.26 | 198.21 | 28.43 | 369.45 | 71.30 | 369.24 | 57.79 |
| 250 | 199.45 | 28.77 | 198.54 | 25.37 | 369.52 | 63.50 | 369.37 | 51.54 |
| 300 | 199.53 | 26.21 | 198.77 | 23.12 | 369.57 | 57.80 | 369.46 | 46.96 |
| 350 | 199.59 | 24.23 | 198.94 | 21.38 | 369.62 | 53.40 | 369.53 | 43.42 |
| 400 | 199.64 | 22.64 | 199.07 | **19.98** | 369.65 | 49.88 | 369.58 | 40.58 |
| 450 | 199.68 | 21.33 | 199.17 | 18.83 | 369.68 | 46.97 | 369.62 | 38.23 |
| 500 | 199.71 | 20.22 | 199.25 | 17.85 | 369.71 | 44.52 | 369.65 | **36.24** |
| 550 | 199.73 | **19.27** | 199.31 | 17.01 | 369.73 | 42.41 | 369.68 | 34.54 |
| 600 | 199.75 | 18.44 | 199.37 | 16.28 | 369.75 | 40.58 | 369.71 | 33.05 |
| 650 | 199.77 | 17.71 | 199.42 | 15.64 | 369.76 | 38.97 | 369.73 | 31.74 |
| 700 | 199.79 | 17.06 | 199.46 | 15.06 | 369.78 | 37.53 | 369.74 | 30.58 |
| 750 | 199.80 | 16.47 | 199.49 | 14.55 | 369.79 | **36.24** | 369.76 | 29.53 |
| 800 | 199.81 | 15.95 | 199.52 | 14.08 | 369.80 | 35.08 | 369.77 | 28.59 |
| ∞ | 200.00 | 0 | 200.00 | 0 | 370.00 | 0 | 370.00 | 0 |

Table 10. AARL(0) and SDARL(0) values for the revised $TS_E$ $\bar{X}$ chart for different number of in-control Phase-I samples ($m$), computed using the optimal parameters of the revised $TS_K$ $\bar{X}$ chart in minimizing AARL(1.5), based on $n_0 \in \{5, 7\}$ and ARL(0) $\in \{200, 370\}$

| $m$ | ARL(0) = 200 | | | | ARL(0) = 370 | | | |
|---|---|---|---|---|---|---|---|---|
| | $n_0 = 5$ | | $n_0 = 7$ | | $n_0 = 5$ | | $n_0 = 7$ | |
| | AARL(0) | SDARL(0) | AARL(0) | SDARL(0) | AARL(0) | SDARL(0) | AARL(0) | SDARL(0) |
| 50 | 187.66 | 85.49 | 184.88 | 69.32 | 342.31 | 180.93 | 348.24 | 174.12 |
| 150 | 194.23 | 47.22 | 193.47 | 39.00 | 356.19 | 99.07 | 359.47 | 95.74 |
| 250 | 196.25 | 36.20 | 195.82 | 29.93 | 360.85 | 75.82 | 363.12 | 73.36 |
| 350 | 197.21 | 30.43 | 196.92 | 25.17 | 363.15 | 63.69 | 364.89 | 61.68 |
| 450 | 197.78 | 26.76 | 197.56 | 22.12 | 364.52 | 55.96 | 365.94 | 54.23 |
| 550 | 198.15 | 24.15 | 197.98 | **19.97** | 365.43 | 50.48 | 366.63 | 48.95 |
| 650 | 198.42 | 22.18 | 198.28 | 18.34 | 366.07 | 46.35 | 367.12 | 44.96 |
| 750 | 198.61 | 20.63 | 198.50 | 17.05 | 366.56 | 43.09 | 367.49 | 41.80 |
| 800 | 198.70 | **19.96** | 198.59 | 16.50 | 366.76 | 41.69 | 367.64 | 40.46 |
| 850 | 198.77 | 19.36 | 198.67 | 16.00 | 366.93 | 40.43 | 367.77 | 39.23 |
| 950 | 198.89 | 18.30 | 198.80 | 15.12 | 367.23 | 38.20 | 368.00 | 37.08 |
| 1000 | 198.94 | 17.83 | 198.86 | 14.73 | 367.36 | 37.22 | 368.10 | **36.13** |
| 1050 | 198.99 | 17.39 | 198.91 | 14.37 | 367.48 | **36.31** | 368.18 | 35.25 |
| 1100 | 199.03 | 16.99 | 198.96 | 14.04 | 367.59 | 35.47 | 368.27 | 34.43 |
| 1150 | 199.07 | 16.61 | 199.00 | 13.73 | 367.68 | 34.67 | 368.34 | 33.67 |
| ∞ | 200.00 | 0 | 200.00 | 0 | 370.00 | 0 | 370.00 | 0 |

Table 11. An implementation of the revised $TS_E$ $\bar{X}$ chart on flow width measurements (in microns) for the Phase-II hard bake process

| Sampling stage, $i$ | Inspection level 1 ($n_1 = 4$) | | | | Inspection level 2 ($n_2 = 3$) | | | Inspection level 3 ($n_3 = 3$) | | | Inspection level 1 | | Inspection level 2 | | | Inspection level 3 | | |
|---|---|---|---|---|---|---|---|---|---|---|---|---|---|---|---|---|---|---|
| | $X_{1i,1}$ | $X_{1i,2}$ | $X_{1i,3}$ | $X_{1i,4}$ | $X_{2i,1}$ | $X_{2i,2}$ | $X_{2i,3}$ | $X_{3i,1}$ | $X_{3i,2}$ | $X_{3i,3}$ | $\bar{X}_{1i}$ | $\widehat{W}_{1i}$ | $\bar{X}_{2i}$ | $Y_{2i}$ | $\widehat{W}_{2i}$ | $\bar{X}_{3i}$ | $Y_{3i}$ | $\widehat{W}_{3i}$ |
| 1 | 1.4483 | 1.5458 | 1.4538 | 1.4303 | | | | | | | 1.4696 | –0.3079 | | | | | | |
| 2 | 1.6206 | 1.5435 | 1.6899 | 1.5830 | 1.3358 | 1.4187 | 1.5175 | | | | 1.6093 | 1.5303 | 1.4240 | 1.5299 | 0.6423 | | | |
| 3 | 1.3446 | 1.4723 | 1.6657 | 1.6661 | | | | | | | 1.5372 | 0.5816 | | | | | | |
| 4 | 1.5454 | 1.0931 | 1.4072 | 1.5039 | 1.5264 | 1.4418 | 1.5059 | | | | 1.3874 | –1.3895 | 1.4914 | 1.4320 | –1.0618 | | | |
| 5 | 1.5124 | 1.4620 | 1.6263 | 1.4301 | | | | | | | 1.5077 | 0.1934 | | | | | | |
| 6 | 1.2725 | 1.5945 | 1.5397 | 1.5252 | | | | | | | 1.4830 | –0.1316 | | | | | | |
| 7 | 1.4981 | 1.4506 | 1.6174 | 1.5837 | | | | | | | 1.5375 | 0.5855 | | | | | | |
| 8 | 1.4962 | 1.3009 | 1.5060 | 1.6231 | | | | | | | 1.4816 | –0.1500 | | | | | | |
| 9 | 1.5831 | 1.6454 | 1.4132 | 1.4603 | | | | | | | 1.5255 | 0.4276 | | | | | | |
| 10 | 1.5808 | 1.7111 | 1.7313 | 1.3817 | 1.3135 | 1.4953 | 1.4894 | | | | 1.6012 | 1.4237 | 1.4327 | 1.5290 | 0.6266 | | | |
| 11 | 1.4596 | 1.5765 | 1.7014 | 1.4026 | | | | | | | 1.5350 | 0.5526 | | | | | | |
| 12 | 1.2773 | 1.4541 | 1.4936 | 1.4373 | | | | | | | 1.4156 | –1.0184 | | | | | | |
| 13 | 1.5139 | 1.4808 | 1.5293 | 1.5729 | | | | | | | 1.5242 | 0.4105 | | | | | | |
| 14 | 1.6738 | 1.5048 | 1.5651 | 1.7473 | 1.6128 | 1.8089 | 1.5513 | 1.8250 | 1.4389 | 1.6558 | 1.6228 | 1.7079 | 1.6577 | 1.6378 | 2.5204 | 1.6399 | 1.6384 | 3.0250 |

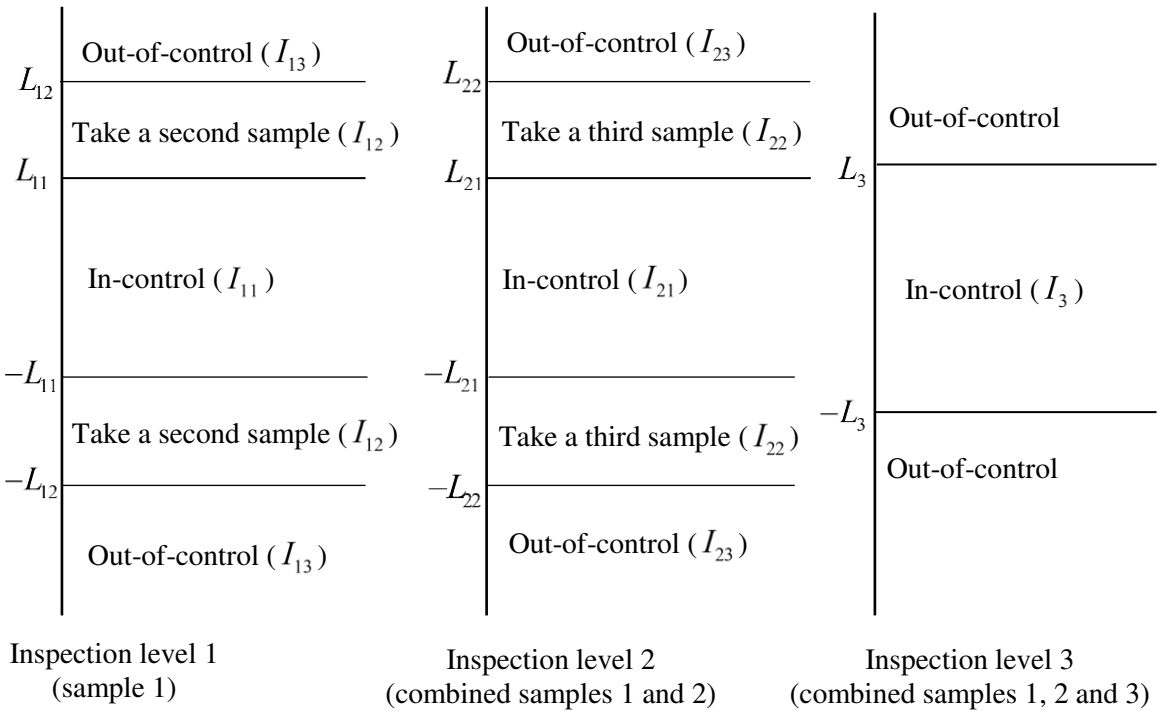


Figure 1. A graphical display of the TS $\bar{X}$ chart

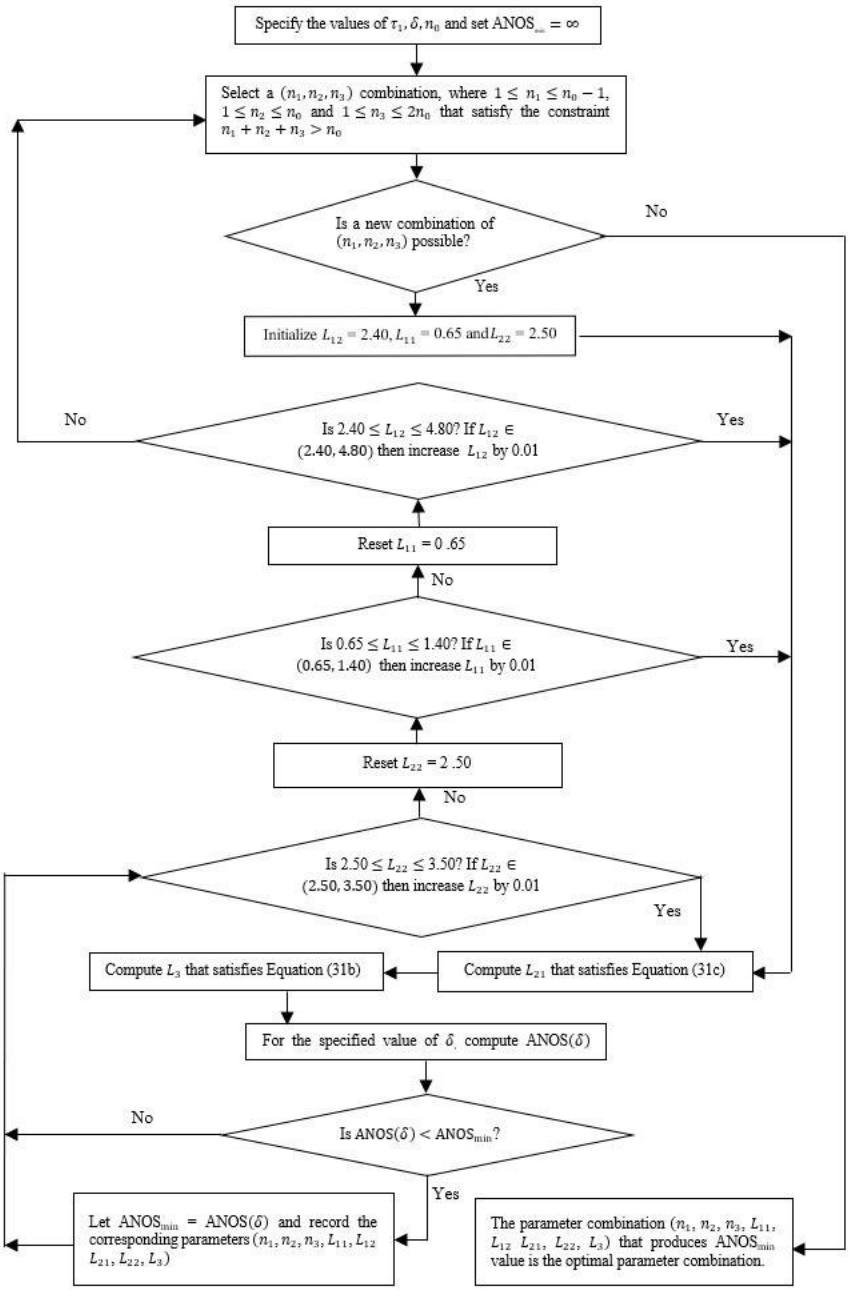


Figure 2. A flow chart for the optimization procedure of the revised $TS_K$ $\bar{X}$ chart in minimizing the value of ANOS($\delta$)

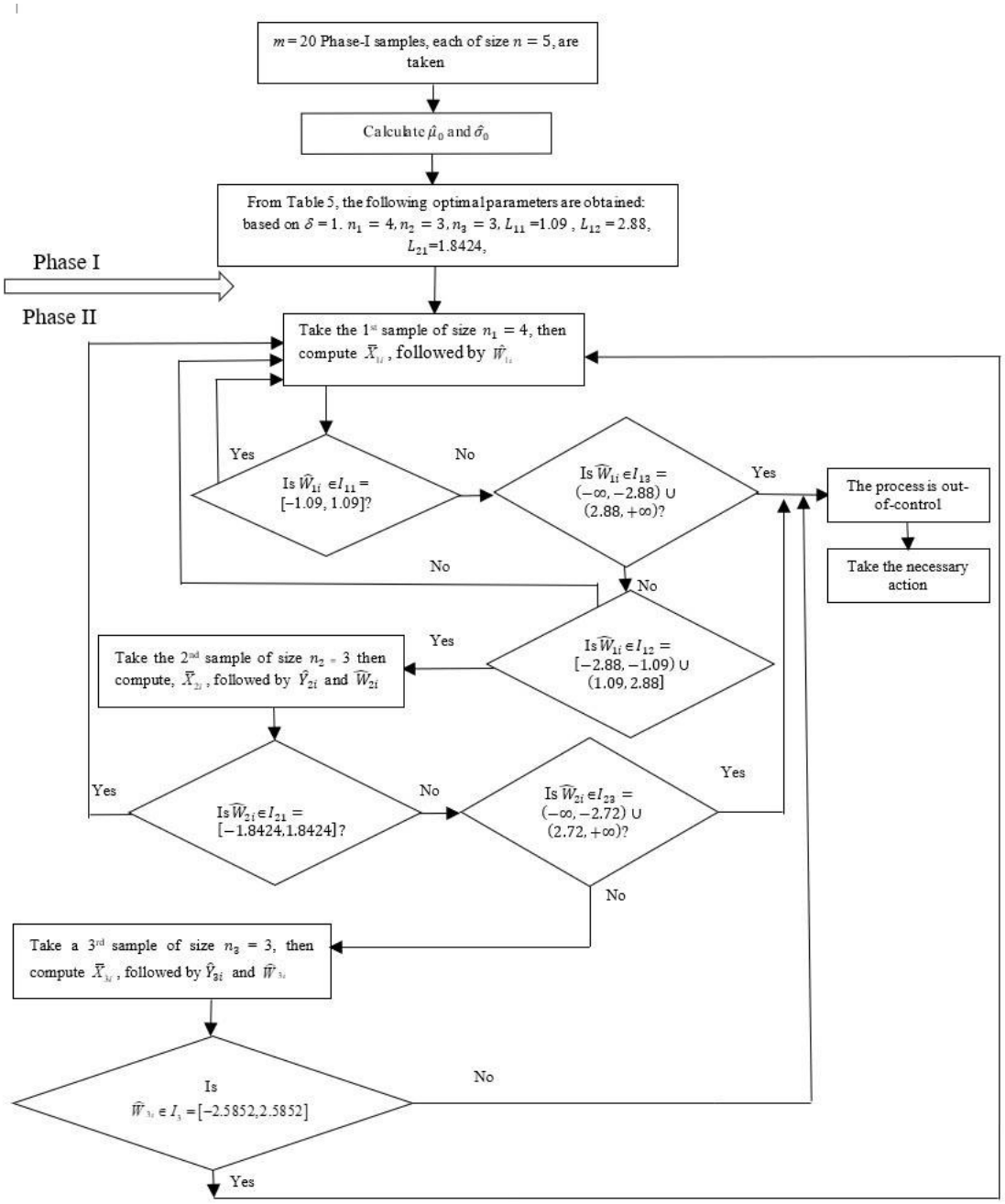


Figure 3. A flow chart in explaining the operation of the revised $TS_E$ $\bar{X}$ chart for the Phase-II process for the monitoring of flow width measurements (in microns) from the hard bake process

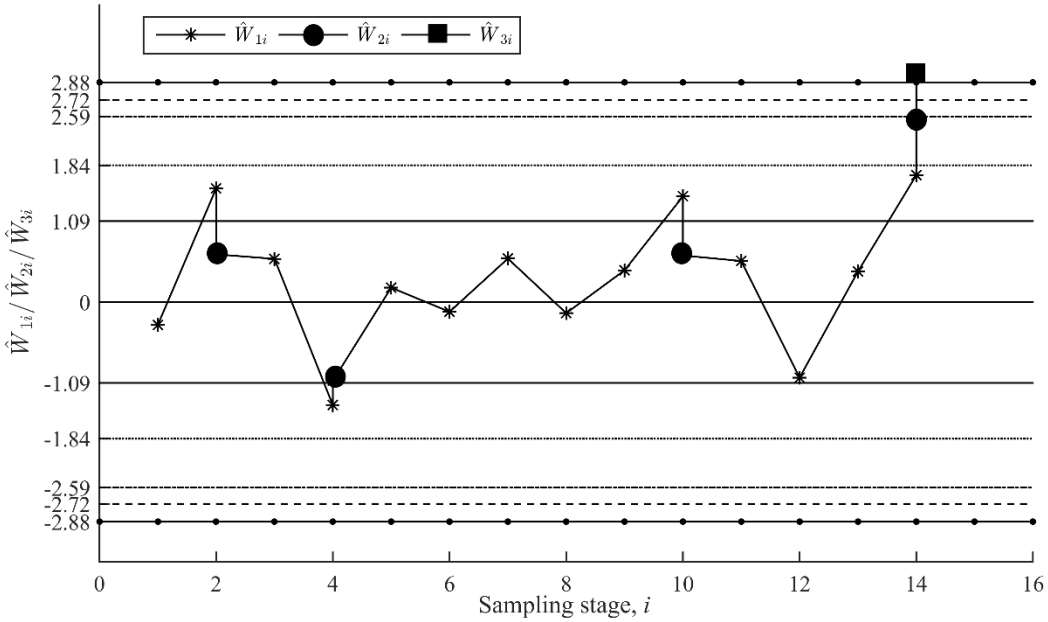


Figure 4. Revised $TS_E$ $\bar{X}$ chart for the Phase-II process for monitoring of flow width measurements (in microns) from the hard bake process